JOURNAL OF GEOPHYSICAL RESEARCH, VOL. 88, NO. B4, PAGES 3295-3314, APRIL 10, 1983

TRAVEL TIMES AND STATION CORRECTIONS FOR P WAVES AT TELESEISMIC DISTANCES

Adam M. Dziewonski

Department of Geological Sciences, Harvard University, Cambridge, Massachusetts 02138

Don L. Anderson

Seismological Laboratory, California Institute of Technology
Pasadena, California 91125

Abstract. Approximately 3300 shallow focus earthquakes and 1000 seismic stations have been used in a study of P wave travel times and station residuals, including azimuthal effects. The events were selected from a catalog containing 160,000 earthquakes, and those having uniform distance and azimuthal coverage were systematically relocated and used to refine P wave travel times and station corrections. Station corrections are provided for 994 seismic stations. The station corrections involve three terms: the static effect and two cosine terms with appropriate phase shifts. They exhibit general consistency over broad geographic areas and, where coverage is dense, often show abrupt changes from one geological province to another. The cos 2θ terms appear to be due to upper mantle anisotropy, and they correlate with the stress direction in the crust.

Introduction

This paper treats a rather traditional topic, one that attracted much attention during the late 1960's and early 1970's, when the high-quality data from the rapidly expanding global seismograph network and fast computers became readily available. Although several papers pointed out inadequacies in the Jeffreys and Bullen [1940] travel times, there were important differences among the travel time curves derived in these studies. Partly for this reason, the National Earthquake Information Service of the U. S. Geological Survey and the International Seismological Centre still use the J-B tables for estimation of hypocentral parameters.

In addition to the practical applications of travel time curves, such as in earthquake location, the inferences drawn from observations of travel times cover a broad range of basic problems in geophysics. Detection of discontinuities and resolution of lateral variations in earth structure are important in understanding dynamic processes within the earth. Station anomalies, including azimuthal effects, can be used to study heterogeneity and anisotropy.

Since arrival times of P waves are the most frequently reported functional of the earth's structure, our ability to process and interpret these data is, in a certain way, a measure of progress in seismology.

The travel times for P waves in the J-B tables are an expansion of the results published by Jeffreys [1939]. In that paper he combined his results on travel times and velocity distribution in the earth which were published in a series of articles dating from 1936 to 1939 in the Geophysical Supplements to the Monthly Notices of the Royal Astronomical Society. The fact that these results are still used as the standard testifies to the excellence of this effort.

The existence of regional variations in travel times had been recognized by Gutenberg [1953], who attributed them primarily to regional changes in the depth of the Mohorovicic discontinuity. Herrin and Taggart [1962] studied regional variations in the P_n travel times in the United States. Carder [1964] used travel times from nuclear explosions and showed that there are significant deviations from the J-B travel times. His results indicated the need for a baseline correction of about -2 s and the existence of distance-dependent residuals. However, Carder used only data from explosions in the Marshall Islands, and the question of a regional bias remained open.

It was the study by Cleary and Hales [1966] that set the stage for most of the later investigations, including this one, that involved globally distributed sets of sources and receivers. The approach adopted by Cleary and Hales is an application of the 'time term' analysis previously used in interpretation of seismic refraction studies [cf. Willmore and Bancroft, 1960]. The objective of this analysis is to represent an observed set of travel times (or residuals) as a sum of source, propagation, and receiver terms. As a result, one obtains an improved set of epicentral coordinates, a new travel time curve, and a set of station corrections. Cleary and Hales were the first to publish an extensive set of station corrections, a parameter that they found to be closely related to the tectonic nature of the receiver region.

Other important papers that involved analysis similar to that of Cleary and Hales are the 1968 Tables [Herrin et al., 1968], the joint epicentre method of Lilwall and Douglas [1970], and the study of travel times for deep earthquakes by Sengupta and Julian [1976].

Dziewonski and Anderson [1981] used a very large set of data (1,500,000 P wave arrival times for 26,000 earthquakes) from the Bulletins of the International Seismological Centre (ISC) for the years 1964 to 1975 to obtain a travel time curve which, together with other subsets of data, was used to derive the Preliminary Reference Earth Model (PREM). However, the epicenters were not relocated in that study, and, as suggested by

Paper number 2B1668.
0148-0227/83/002B-1668$05.00

A. Douglas (personal communication, 1981), some residual effect of the J-B curve might have remained.

Other studies included dT/dΔ measurements using seismic arrays [cf. Niazi and Anderson, 1965; Johnson, 1967, 1969; Toksöz et al., 1967; Chinnery, 1969] and the search for the lateral heterogeneity in the mantle [cf. Julian and Sengupta, 1973; Dziewonski et al., 1977]. These papers have a bearing on the subject of this report, but our present purpose is to use the data for shallow earthquakes contained in the bulletins for the years 1964-1978 in order to clarify several issues that are still controversial.

The shape of the travel time curve. The principal difference between the results of Cleary and Hales [1966], Herrin et al. [1968], and Lilwall and Douglas [1970] was the slope of the travel time curve. The largest difference exists between the first two studies: between 30° and 90° the slowness of the 1968 tables is greater by 0.023 s/deg than that inferred by Cleary and Hales. There are also differences in the details of the travel time curves. Even though these differences do not exceed 0.3 s, they ought to be resolvable.

The question of the source bias. Most of the earthquakes (~ 80%) occur at or near subduction zones. Because of the velocity structure in the subducted slab, travel time residuals tend to have very particular patterns [cf. Davies and McKenzie, 1969]. A desire to avoid this effect motivated the study of Sengupta and Julian [1976]. However, if the effect of the slab extends below 700 km [Jordan, 1977], then the use of only deep-focus earthquakes not only does not free one from source bias but also severely restricts the geographical coverage.

Azimuthal dependence of station corrections. Herrin and Taggart [1968] and Lilwall and Douglas [1970] evaluated station correction terms that, in addition to the constant term, provided for a sinusoidal variation with azimuth (plus a constant phase term). Sengupta and Julian [1976] found that the correlation coefficient between these two sets of azimuth-dependent corrections was 0.41. This figure indicates contamination by noise or uneven coverage. Figure 3 of Herrin and Taggart [1968] indicates that while there is overall consistency among the slow direction vectors in the eastern United States, the magnitude and direction of these vectors are highly incoherent in the central and western United States.

Our objective is to demonstrate that by using a significantly larger set of data and an approach to estimation of the azimuth-dependent terms that accounts for the uneven distribution of observations as a function of azimuth, it is possible to demonstrate regional coherence of not only the first but also the second azimuthal term.

The Data Set

The ISC Bulletins for the years 1964-1978 contain entries for approximately 160,000 earthquakes. Most of these events are small with relatively few reports of arrival times by individual stations. For the purpose of our study we require events for which stable epicenters can be determined using only the teleseismic travel times. Thus we have scanned the ISC tapes for earthquakes that had at least 30 arrival times between 30° and 90° of epicentral distance and at least five readings in each azimuthal quadrant. This search yielded 3270 events.

As discussed in the introduction, the effect of source bias in the vicinity of subducted slabs is a subject of concern. Subduction-related events dominate the catalog even though trenches cover a relatively small fraction of the earth's surface. In order to avoid as well as to study this bias, we divide the selected sources into two classes: class I, events away from subduction zones; and class II, events in the vicinity of subduction zones.

Figure 1 shows the geographical distribution of the two classes of events. The symbols indicate that at least one event of a particular class occurred within a given 5° x 5° cell; circles designate class I events; stars, class II. Even though there are 3 times more class II events, class I earthquakes occupy roughly twice as many cells and provide more uniform coverage of the earth's surface. For this reason the class I events are considered the primary data; class II earthquakes are processed separately.

In the last stage of the entire process, when the station corrections are determined, the condition of the azimuthal coverage of an event is relaxed: three azimuthal quadrants must contain at least five observations. This triples the number of available events and improves the azimuthal coverage of the individual stations. A number of precautions are taken that this does not introduce a bias.

There are over 1000 stations that reported 30 or more arrival times within the established range of epicentral distance. At least one component of the station correction can be established for most of these stations.

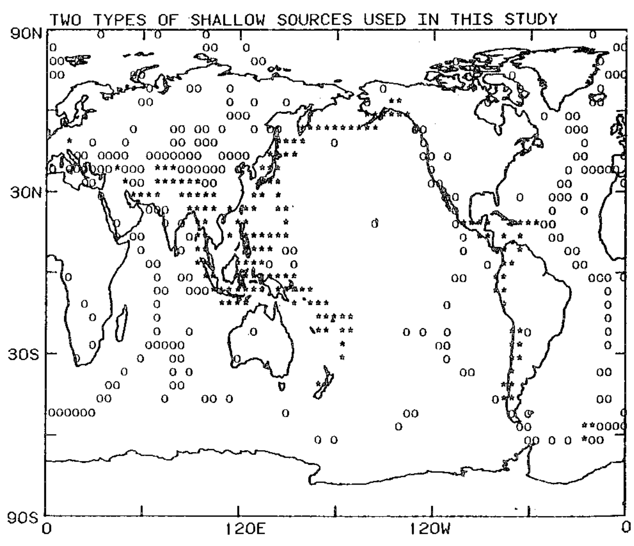

Fig. 1. Distribution of shallow sources used in this study. A symbol indicates that at least one event for a given 5° x 5° cell was used in the analysis. Circles designate class I events; stars, class II events: earthquakes that occur near or at subduction zones.

The Iterative Time Term Analysis

The time term method, as described by Cleary and Hales [1966], is based on the following equation of condition:

$$\delta t_{ij} = a_{ij} + b_j + d_i \quad (1)$$

where for the ith station and jth earthquake, δt is the observed residual from the reference travel time curve; a is the perturbation to the travel time curve for the particular source-receiver pair; b is the source term and d is the station term.

Cleary and Hales assumed that a_{ij} is a function of distance only: $a_{ij} = a_k(\Delta_{ij})$, where k is an integer selected such that it covers a 2° cell. The same division has been assumed by Lilwall and Douglas [1970] and Sengupta and Julian [1976]; a 1° cell size was adopted by Herrin et al. [1968] and in this study. In general, the term a may depend on the geographical coordinates of the source and receiver; this formulation was used by Dziewonski et al. [1977] in a search for large scale velocity heterogeneities in the mantle. In this case a_{ij} is represented by a product of unknown structural parameters with the appropriate kernels.

Cleary and Hales represented the source term b by a constant, essentially a perturbation in the origin time. The events were relocated after each iteration. In general, the source term can be associated with a perturbation in the hypocentral coordinates of the source. In this case, b is equivalent to the product of a matrix of partial derivatives with the vector of perturbations in hypocentral parameters. Lilwall and Douglas [1970] adopted this approach with the source depth fixed.

Cleary and Hales represented the station term d by a constant. In general it may be azimuth dependent:

$$d_{ij} = \sum_{n=0}^{N} C_{in} \cdot \cos n\xi_{ij} + S_{in} \cdot \sin n\xi_{ij}$$

where ξ_{ij} is the azimuth from the ith station to the jth source. Herrin et al. [1968] and Lilwall and Douglas [1970] considered N = 1; in this study, N varies between 0 and 2, depending on the azimuthal coverage at the station.

There is a natural nonuniqueness in (1); clearly, the same amount of time may be added to all a_{ij} and subtracted from all d_i and the observed value δt_{ij} would remain unchanged. Therefore it is necessary to fix arbitrarily one value of the a parameter and one value of the station correction. Provided that this is done, application of the least squares condition to the set of equations of condition (1) leads to a system of normal equations:

$$\underline{A} \cdot \underline{x} = \underline{B} \quad (2)$$

The matrix $\underline{A}$ has the structure

$$\underline{A} = \begin{bmatrix} C & H & G \\ H & D & F \\ G & F & E \end{bmatrix} \quad (3)$$

where C, D, and E are diagonal or block diagonal matrices. If C is associated with the travel time corrections that depend only on epicentral distance, then it is diagonal; if D is associated with the source term, then it is diagonal in the formulation of Cleary and Hales or (3 x 3) block diagonal in the case of Lilwall and Douglas. Matrix E is block diagonal with block dimensions of (2N + 1); E is diagonal for N = 0. Matrices F, G, and H are the cross-product matrices; in the case considered by Cleary and Hales they have the property that all their elements are positive integers and the sum of a given row or column is equal to the appropriate diagonal element.

If, as in this study, we consider 2000 events to be relocated, 1000 stations with an average of three unknowns per station to be determined and travel time corrections to be determined for 76 epicentral distance cells, the matrix A would have dimensions of the order of 9000 x 9000. Computation of the inverse of such a matrix is impractical even using the largest available computers.

However, the fact that matrix A is dominated by its diagonal submatrices C, D, and E, allows us to initiate an iterative procedure that does not require an explicit evaluation of the inverse of A.

If we approximate the inverse of A by

$$\underline{\tilde{A}}^{-1} = \begin{bmatrix} C^{-1} & & 0 \\ & D^{-1} & \\ 0 & & E^{-1} \end{bmatrix} \quad (4)$$

then the first approximation of the unknown vector $\underline{x}$ is

$$\underline{x}_{(0)} = \underline{\tilde{A}}^{-1}_{(0)} \cdot \underline{B}_{(0)} \quad (5)$$

This is equivalent to (1) estimation of the correction to the travel times by averaging the residuals with respect to the starting travel time curve, (2) relocation of the individual events using the starting travel time curve, and (3) estimation of station corrections for the individual stations.

In the next iteration, we evaluate

$$\begin{aligned} \delta\underline{x}_{(1)} &= \underline{\tilde{A}}^{-1}_{(1)} \cdot (\underline{B}_{(0)} - \underline{A}_{(1)} \cdot \underline{x}_{(0)}) = \underline{\tilde{A}}^{-1}_{(1)} \cdot \underline{B}_{(1)} \\ \underline{x}_{(1)} &= \underline{x}_{(0)} + \delta\underline{x}_{(1)} \end{aligned} \quad (6)$$

or, in general,

$$\begin{aligned} \delta\underline{x}_{(n)} &= \underline{\tilde{A}}^{-1}_{(n)} \cdot \underline{B}_{(n)} \\ \underline{x}_{(n)} &= \underline{x}_{(n-1)} + \delta\underline{x}_{(n)} \end{aligned} \quad (7)$$

If the inverse of matrix A is stable, then the iterative process described above should converge. This means that, formally, the procedure adopted by Lilwall and Douglas [1970] on the one hand and Herrin et al. [1968], Sengupta and Julian [1976], and this study on the other are equivalent; the procedure of Cleary and Hales [1966] falls between the two approaches. Thus the differences in the final results must be explained by the selection of events and stations rather than by the specific algorithm adopted.

For practical reasons (the process of estimation of station residuals is very time consuming) we depart somewhat from the iterative procedure described above. Each cycle consists of (1) relocation of events, (2) determination of improved travel time curve, and (3) estimation of station corrections. We repeat steps 1 and 2 until convergence is achieved and only then evaluate station correction. The cycle is then repeated. To verify that this departure from the ideal procedure does not introduce a bias, we have carried out the entire process having in the first step calculated station corrections using the J-B travel times and the original ISC locations. The difference in the final results was negligible.

The Procedure and Results

Given a travel time curve and starting locations, relocation of a hypocenter is routine: an exhaustive description can be found, for example, by Tucker et al. [1968]. Ellipticity corrections were introduced using the formula and tabular values given by Dziewonski and Gilbert [1976].

Because the azimuthal distribution of stations with respect to the epicenter tends to be uneven, we have tested a weighting scheme in which, regardless of the number of observations, each azimuthal quadrant was given equal weight. In terms of the average travel time curve for the total set of either class I or class II events, that weighting approach did not change the results by more than 0.02-0.03 s. We have not investigated what effect this weighting scheme had on location of the individual events, but, in general, individual events were not of interest in this study. Another test was performed by relaxing the condition on the azimuthal coverage: only three azimuthal quadrants were required to have not less than five observations. This allowed us to triple the amount of available data. Again, the effect on the average travel time curve was negligible; other than that the increased amount of data resulted in a somewhat smoother residual curve.

In the relocation procedure it is necessary to have a differentiable travel time curve. The perturbations obtained in each iteration were fit with cubic splines with three knots. This representation was sufficient to avoid any significant long-term deviations between the observed and smoothed curves.

Figure 2 shows, in terms of deviations from the 1968 travel times, the starting curve, one obtained in the first iteration and the final one (after four iterations). It is clear that most of the change occurs in the first iteration. As stated earlier, the class I events are considered the principal data set. Therefore class II events are relocated also using the class I travel time curve. It is clear from Figure 2 that there are some differences between the travel times for class I and class II events. Both curves, however, are relatively close to the 1968 tables, with the curve for class II events being closer and showing only a slight offset in the baseline and slope. This is not surprising, since some 80% of the events used in the derivation of the 1968

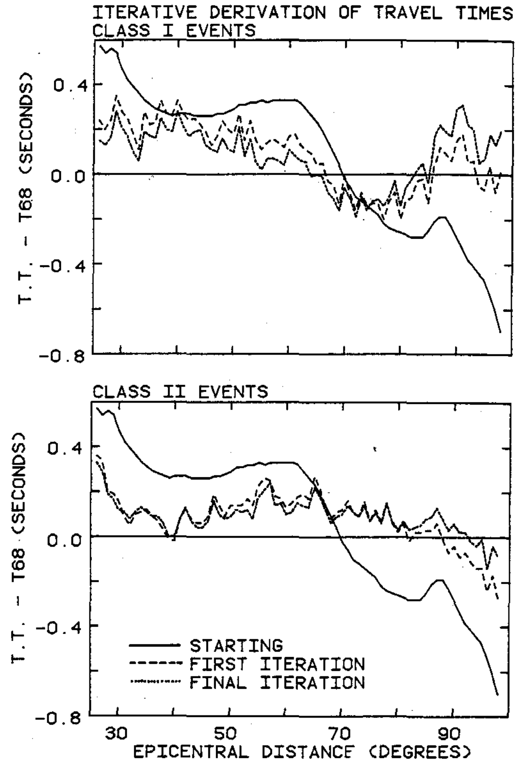

Fig. 2. Illustration of the convergence of iterative derivation of teleseismic travel times for P waves. The results are displayed as residuals with respect to 1968 tables. Station corrections are not yet included.

tables were class II events [see Herrin et al., 1968, Figure 3].

After the convergence of travel times is achieved, the residuals are sorted by station, and the process of determination of station corrections begins. The full azimuth range is divided into 18 windows, 20° wide. An average residual is calculated if there are at least five readings in a given window. From now on, these average residuals are treated with equal weight; this reduces the bias due to unequal distribution of events [see Herrin and Taggart, 1968, Figure 1]. In general, the least squares approach is used to determine the coefficients A and B in the equation

$$\delta t = A_0 + A_1\cos\xi + B_1\sin\xi + A_2\cos2\xi + B_2\sin2\xi \quad (8)$$

However, the number of terms to be determined depends on the azimuthal coverage at a given station. All terms are determined if the data exist for 15 or more windows. Below that number, decisions are made depending on the distribution of the missing windows and the pattern of deviations; admittedly, some decisions are subjective. Station corrections are not determined if data are available for fewer than two windows.

Figure 3 shows a plot of station residuals as a function of azimuth. It is one of the final plots, but it serves well to explain the interactive process of determination of station corrections. The squares are residuals for the class I events; stars are for class II. Averages

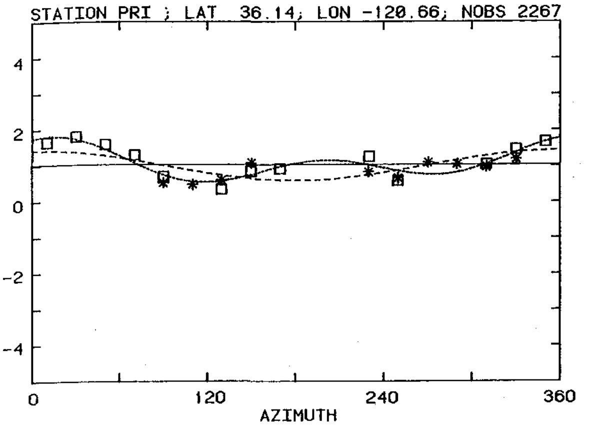

Fig. 3. Station residuals as a function of azimuth. Square represents an average of all residuals for class I events within a given 20° window; stars correspond to class II events. Solid line is the least squares fit of the constant term; long-dashed line, constant and first azimuthal term; short-dashed line, constant and two azimuthal terms.

for individual windows are given equal weight. The straight, solid line is the A_0 term: the average of all residuals. The long-dashed line corresponds to the least squares fit of the first three terms in equation (8). Finally, the short-dashed line represents all five terms. The coverage by class I events is more complete; it would have been possible to determine all five terms even if the data for class II events were not included, and the derived parameters would differ little from those shown. On the other hand, even though there are class II data for 10 out of 18 windows, fitting of terms other than A_0 would not be justified, as the data are very unevenly distributed. Overall, in windows for which both kinds of data exist, the average residuals for both classes of events are very close, indicating that the source term, at least for this station, is not very important or has been absorbed in the relocation of the epicenters. This seems to be the case for most stations.

The stations corrections were computed using three sets of relocated earthquakes: (1) class I data: four quadrants with at least five observations, (2) class I and II data: four quadrants with at least five observations, and (3) class I and II data: three quadrants with at least five observations.

Clearly, the number of data for each of the subsequent sets increases, and yet, whenever a comparison could be made, the results obtained using sets 1 and 3 were fully compatible. For this reason we use set (3) to evaluate station corrections, since it allows us to investigate more stations with a better azimuthal coverage.

In the next cycle, the events are relocated using station corrections, and after two more iterations, convergence of the travel time curves is achieved. The next set of station corrections differs insignificantly from the previous one, and we conclude that the process has converged.

Our main interest in this study was the derivation of station residuals and a new average travel time curve for distances beyond 25°. However, with the relocated earthquakes and available readings at shorter distances we can also construct an average travel time curve from 1° to 25°. Although regional variations become important at these distances, the usefulness of the new travel times is enhanced by having available values for the full range of distances. We remind the reader that only tha data between 30° and 90° were used in the process of relocation of events and estimation of station corrections.

As before, we construct average travel times for 1° cells and then smooth them with a set of polynomials with various conditions of continuity at the knots. The smoothed travel times are continuous throughout, but the first derivative (slowness) was allowed to be discontinuous at 18° and 24°. Except for the distance from 18° to 24° and from 90° to 100°, where a quadratic was fitted, cubic polynomials were used in the remaining segments (1°-18°, 24°-40°, 40°-65°, 65°-90°). The rms of the fit improves with increasing epicentral distance. For the class I travel time curve it is 0.44 s between 1° and 18°, 0.11 s between 18° and 24°, 0.06 s bewteen 24° and 40°, and beyond this distance it ranges from 0.04 to 0.05 s.

Our final average travel times are given in Table 1. Tabulated are epicentral distance (DEL), number of observations (NOBS), average travel time (TOBS), standard deviation of single observation (S.D.), smoothed travel time (TCOM), difference between observed and smoothed values (DIFF), and slowness (DT/DD) in seconds/degree. Travel times for both class I and class II events are given; the maximum difference between smoothed values for the two sets is 0.12 s between 90° and 94°.

Table 2 contains stations corrections for 994 stations. Most of the entries are self-explanatory. NW is the number of 20° azimuth windows for which data were available; RMS0 is the rms error calculated after the A_0 term is removed from averages for individual windows; RMS1 is the error after the higher-order terms (if any) have been removed. The station correction term (to be added to the theoretical travel time) has the form

$$\delta t = A0 + A1 \cdot \cos(\xi - E1) + A2 \cdot \cos 2(\xi - E2)$$

Thus the azimuths E1 and E2 represent the slow directions. For the second azimuthal term there is another slow direction: E2 + 180°.

Discussion

Figure 4 shows a comparison of the residual travel time curves for the class I and class II events before and after introduction of station corrections. There are several important conclusions that can be drawn from this figure.

The average number of observations for a 1° cell is about 1600 for the class I data and 4000 for the class II data. With an rms of single observation of 1.2 s, the standard error of the mean (sem) for the class I data should be 0.03 s and 0.02 for the class II data. The roughness in the uncorrected class I curve exceeds only slightly what could be considered random scatter.

TABLE 1. Final Travel Times and dt/dΔ for Class I and Class II Events

DEL	CLASS I EVENTS						CLASS II EVENTS					
	NOBS	TOBS	S.D.	TCOM	DIFF	DT/DD	NOBS	TOBS	S.D.	TCOM	DIFF	DT/DD
1	73	18.13	1.54	18.66	-0.53	14.440	1488	19.29	1.78	19.51	-0.22	14.177
2	177	33.50	1.92	33.06	0.44	14.349	2495	33.87	1.75	33.67	0.20	14.133
3	182	47.68	1.90	47.36	0.32	14.258	2582	47.90	1.81	47.78	0.12	14.084
4	203	61.23	2.00	61.57	-0.34	14.167	2375	61.42	1.82	61.84	-0.42	14.032
5	240	76.01	1.92	75.70	0.31	14.076	2684	76.16	2.04	75.84	0.32	13.975
6	263	90.25	2.22	89.73	0.52	13.986	2301	90.06	2.15	89.78	0.28	13.913
7	307	103.16	2.04	103.67	-0.51	13.895	1859	103.54	2.13	103.66	-0.12	13.848
8	375	118.16	1.99	117.52	0.64	13.804	1749	118.18	2.01	117.48	0.70	13.778
9	559	130.32	2.13	131.27	-0.95	13.712	1922	130.55	2.12	131.22	-0.67	13.704
10	534	144.62	2.23	144.94	-0.32	13.621	1829	144.54	2.10	144.88	-0.34	13.625
11	648	158.12	2.22	158.52	-0.40	13.530	1552	158.12	2.18	158.47	-0.35	13.543
12	629	172.56	2.18	172.00	0.56	13.439	1321	172.34	2.12	171.97	0.37	13.456
13	780	185.18	2.18	185.40	-0.22	13.348	1366	184.90	2.15	185.38	-0.48	13.365
14	753	199.12	2.24	198.70	0.42	13.257	1189	199.07	2.14	198.69	0.37	13.269
15	937	212.11	2.21	211.91	0.20	13.165	1279	212.02	2.10	211.91	0.11	13.169
16	910	225.12	2.12	225.03	0.09	13.074	1562	225.39	2.07	225.03	0.36	13.065
17	1177	238.15	2.15	238.06	0.09	12.982	1636	238.22	2.01	238.04	0.18	12.956
18	1220	250.78	1.96	250.99	-0.21	12.891	1745	250.68	1.91	250.94	-0.26	12.844
18	1220	250.78	1.96	250.99	-0.21	11.522	1745	250.68	1.91	250.94	-0.26	11.672
19	1328	262.45	1.77	262.38	0.07	11.252	2077	262.56	1.76	262.46	0.10	11.360
20	1303	273.66	1.69	273.50	0.16	10.981	2197	273.82	1.70	273.66	0.16	11.047
21	1384	284.31	1.40	284.34	-0.03	10.711	2437	284.53	1.64	284.55	-0.02	10.735
22	1531	294.80	1.48	294.92	-0.12	10.440	2434	294.96	1.68	295.13	-0.17	10.423
23	1453	305.14	1.54	305.22	-0.08	10.170	2510	305.37	1.65	305.40	-0.03	10.110
24	1596	315.18	1.42	315.26	-0.08	9.899	2471	315.30	1.63	315.35	-0.05	9.798
24	1596	315.18	1.42	315.26	-0.08	9.267	2471	315.30	1.63	315.35	-0.05	9.247
25	1634	324.60	1.40	324.49	0.11	9.205	2319	324.62	1.57	324.57	0.05	9.187
26	1568	333.85	1.44	333.67	0.18	9.143	2364	333.96	1.52	333.73	0.23	9.128
27	1499	342.88	1.49	342.78	0.10	9.081	2396	342.92	1.46	342.83	0.09	9.069
28	1477	351.92	1.45	351.83	0.09	9.020	2312	351.87	1.40	351.86	0.00	9.010
29	1547	360.87	1.27	360.82	0.05	8.959	2509	360.78	1.42	360.85	-0.07	8.951
30	1403	369.72	1.29	369.75	-0.03	8.899	2613	369.69	1.38	369.77	-0.08	8.893
31	1534	378.51	1.24	378.62	-0.11	8.839	2603	378.59	1.36	378.63	-0.04	8.835
32	1537	387.25	1.20	387.43	-0.18	8.780	2903	387.35	1.31	387.44	-0.09	8.777
33	1479	396.07	1.17	396.18	-0.11	8.721	2801	396.19	1.24	396.19	0.01	8.719
34	1536	404.79	1.17	404.87	-0.08	8.663	2701	404.88	1.30	404.88	0.01	8.661
35	1724	413.51	1.23	413.50	0.00	8.605	2708	413.49	1.30	413.51	-0.02	8.604
36	1811	422.12	1.20	422.08	0.04	8.548	2923	422.09	1.29	422.08	0.01	8.547
37	2012	430.65	1.16	430.60	0.05	8.491	3034	430.58	1.25	430.60	-0.02	8.490
38	1697	439.16	1.15	439.06	0.10	8.435	3104	439.11	1.28	439.06	0.05	8.433
39	1746	447.54	1.19	447.47	0.07	8.379	3446	447.49	1.28	447.47	0.02	8.377
40	1915	455.89	1.20	455.82	0.07	8.323	3467	455.84	1.28	455.81	0.02	8.320
41	2003	464.11	1.09	464.11	0.00	8.248	3568	464.13	1.29	464.10	0.03	8.245
42	1759	472.30	1.12	472.32	-0.02	8.172	3433	472.32	1.20	472.31	0.01	8.171
43	1689	480.43	1.22	480.45	-0.02	8.097	3669	480.45	1.27	480.44	0.01	8.096
44	1923	488.51	1.15	488.51	-0.00	8.022	3503	488.49	1.26	488.50	-0.01	8.022
45	1987	496.46	1.15	496.50	-0.04	7.947	3582	496.48	1.19	496.48	-0.00	7.948
46	1917	504.34	1.17	504.41	-0.07	7.873	3580	504.37	1.22	504.40	-0.03	7.875
47	2131	512.12	1.15	512.24	-0.12	7.799	3685	512.26	1.21	512.23	0.03	7.801
48	1837	519.99	1.13	520.00	-0.01	7.725	3525	519.96	1.23	520.00	-0.04	7.728
49	1813	527.69	1.19	527.69	-0.00	7.652	3910	527.65	1.17	527.69	-0.04	7.655
50	1793	535.28	1.11	535.31	-0.03	7.579	3830	535.31	1.16	535.31	0.00	7.583
51	1647	542.92	1.16	542.85	0.07	7.506	3724	542.85	1.20	542.86	-0.01	7.510
52	1812	550.31	1.23	550.32	-0.01	7.433	3328	550.31	1.18	550.33	-0.02	7.438
53	1916	557.77	1.23	557.72	0.05	7.361	3548	557.73	1.21	557.73	-0.00	7.366
54	1916	565.10	1.20	565.04	0.06	7.289	3871	565.02	1.19	565.06	-0.04	7.295
55	1965	572.32	1.18	572.29	0.02	7.217	3916	572.34	1.17	572.32	0.02	7.223
56	1954	579.49	1.21	579.48	0.01	7.146	3702	579.55	1.14	579.51	0.04	7.152
57	1826	586.59	1.18	586.59	0.00	7.075	3773	586.65	1.17	586.63	0.02	7.081
58	1933	593.66	1.15	593.63	0.03	7.004	4110	593.67	1.13	593.67	-0.00	7.011
59	1902	600.57	1.14	600.59	-0.03	6.934	4320	600.65	1.13	600.65	0.00	6.940
60	1866	607.51	1.17	607.49	0.02	6.863	4137	607.57	1.17	607.55	0.02	6.870
61	1743	614.32	1.26	614.32	-0.00	6.794	4170	614.40	1.13	614.39	0.01	6.800
62	1724	621.04	1.20	621.08	-0.04	6.724	4400	621.15	1.15	621.15	-0.00	6.731
63	1674	627.74	1.16	627.77	-0.03	6.655	4581	627.80	1.14	627.85	-0.05	6.661
64	1629	634.43	1.19	634.39	0.04	6.586	4730	634.44	1.15	634.48	-0.04	6.592
65	1698	640.92	1.14	640.94	-0.02	6.517	4676	641.07	1.15	641.03	0.04	6.523
66	1619	647.39	1.20	647.42	-0.03	6.446	4699	647.54	1.10	647.52	0.02	6.450
67	1542	653.86	1.19	653.83	0.03	6.376	4661	653.96	1.10	653.93	0.03	6.377
68	1548	660.13	1.18	660.18	-0.04	6.305	5019	660.24	1.13	660.27	-0.03	6.304
69	1481	666.40	1.14	666.44	-0.04	6.233	5046	666.53	1.13	666.54	-0.01	6.230
70	1600	672.64	1.21	672.64	-0.00	6.161	5351	672.75	1.13	672.73	0.02	6.156
71	1478	678.80	1.27	678.77	0.03	6.089	5544	678.87	1.11	678.85	0.02	6.082
72	1586	684.79	1.21	684.82	-0.03	6.016	5726	684.89	1.12	684.90	-0.01	6.008
73	1498	690.86	1.24	690.80	0.06	5.943	5472	690.85	1.09	690.87	-0.02	5.934
74	1484	696.64	1.14	696.71	-0.06	5.870	5705	696.72	1.11	696.77	-0.05	5.859
75	1505	702.58	1.21	702.54	0.04	5.796	5597	702.57	1.11	702.59	-0.02	5.785
76	1614	708.34	1.21	708.30	0.04	5.722	6358	708.36	1.10	708.34	0.02	5.710
77	1567	713.98	1.17	713.98	-0.00	5.648	6729	714.00	1.10	714.01	-0.01	5.635
78	1411	719.56	1.15	719.59	-0.03	5.573	7858	719.61	1.11	719.60	0.01	5.559
79	1335	725.20	1.28	725.13	0.07	5.498	8261	725.12	1.07	725.13	-0.01	5.484
80	1448	730.60	1.20	730.59	0.01	5.422	8215	730.54	1.13	730.57	-0.03	5.408
81	1496	736.00	1.15	735.97	0.03	5.346	8296	735.96	1.13	735.94	0.02	5.332
82	1523	741.28	1.18	741.28	0.00	5.270	8238	741.26	1.10	741.24	0.02	5.256
83	1367	746.54	1.20	746.51	0.03	5.193	7810	746.50	1.11	746.46	0.04	5.180
84	1476	751.68	1.22	751.66	0.02	5.116	7962	751.66	1.12	751.60	0.06	5.104
85	1454	756.64	1.18	756.74	-0.10	5.038	7523	756.68	1.13	756.66	0.02	5.027
86	1498	761.74	1.29	761.74	-0.00	4.961	7122	761.64	1.15	761.65	-0.01	4.950
87	1320	766.72	1.32	766.66	0.06	4.882	6280	766.56	1.17	766.56	-0.00	4.873
88	1369	771.45	1.23	771.51	-0.06	4.804	5486	771.35	1.23	771.40	-0.05	4.796
89	1264	776.18	1.23	776.27	-0.09	4.725	5117	776.07	1.23	776.16	-0.09	4.719
90	1222	780.97	1.25	780.96	0.01	4.646	4758	780.83	1.28	780.84	-0.01	4.641
91	1306	785.55	1.14	785.59	-0.04	4.632	4564	785.47	1.28	785.47	-0.00	4.630
92	976	790.16	1.25	790.22	-0.06	4.618	3921	790.12	1.27	790.10	0.02	4.618
93	850	794.91	1.32	794.83	0.08	4.604	3661	794.77	1.34	794.71	0.06	4.606
94	822	799.49	1.33	799.43	0.06	4.590	3446	799.31	1.37	799.31	0.00	4.595
95	670	803.93	1.39	804.01	-0.08	4.577	3124	803.90	1.42	803.90	0.00	4.583
96	620	808.67	1.57	808.58	0.09	4.563	2868	808.45	1.43	808.48	-0.02	4.571
97	499	813.14	1.54	813.14	0.00	4.549	2430	813.04	1.46	813.04	-0.00	4.560
98	485	817.71	1.50	817.68	0.03	4.535	2280	817.60	1.48	817.59	0.01	4.548
99	397	822.20	1.57	822.21	-0.01	4.522	2050	822.14	1.47	822.14	0.00	4.536
100	338	826.68	1.58	826.72	-0.04	4.508	1751	826.66	1.48	826.67	-0.01	4.524

TOBS are 1° cell means; TCOM are smoothed travel times.

However, for the uncorrected class II curve, excursions from a smooth line are 2-3 times larger than the sem. These excursions tend to extend over several adjacent cells and might suggest minor discontinuities in the lower mantle. The difference between the class I and class II curves reaches nearly 0.3 s between 70° and 80°, implying statistically significant differences between the two data sets.

These inferences were made assuming that the errors are random. There were some 3300 events that contributed to these averages and over 1000 stations reporting some 350,000 P wave arrival times. It is difficult to keep track of such a large amount of data, and one would feel justified in assuming that the data set has been randomized.

The bottom part of Figure 4 proves that this assumption is incorrect. Introduction of station corrections (which are primarily determined from the class I data because of the more uniform geographical distribution) diminished the rms error of a single observation by only 10%, on average. The effect of station corrections on the class I curve is significant but relatively modest in comparison with the effect on the class II curve. Many large excursions have nearly vanished, leading to a much smoother curve. On the other hand a large, long-wavelength depression between 70° and 90° has been added, bringing class I and class II travel times very close to each other. Between 30° and 85° the differences do not exceed 0.1 s.

In view of the effect that station corrections had on both curves, it would be difficult to defend an argument in favor of major, global scale discontinuities in the lower mantle between a depth of some 800 km and the top of the D" layer. The residual roughness of these curves seems to be uncorrelated. Considering the crudeness of the station corrections (e.g., lack of distance dependence), the remaining differences could be explained by their inadequacy, even though the differences may appear to be statistically significant. The detection of lower mantle discontinuities will probably require detailed studies of waveforms since the travel time anomalies, if any, are very small.

At this point it may be worthwhile to quote Jeffreys [1939, p. 506], including a charming footnote:

> It seems to be necessary to insist again that a standard error is not a final claim of any specified degree of accuracy. It is always subject to the condition that no unforseen complications may be present; but the onus of proof is on the advocate of such complications, and they must be stated in a form leading to verifiable inferences before they can be discussed.*

And the footnote is

> *Otherwise we are in Alice's position in her conversation with the Cheshire Cat: 'Which way ought I to go to get from here?' 'That depends a good deal on where you want to get to' said the Cat. 'I don't much care where...' said Alice. 'Then it doesn't matter which way you go,' said the Cat.

TABLE 2. Station Corrections

CODE	LAT	LONG	ELEV	P-WAVE STATION CORRECTION NOBS	NW	RMS0	RMS1	A0	A1	E1	A2	E2
AAA	43.272	76.947	800	31	2	0.46		0.80				
AAB	43.267	77.383	850	2917	17	0.58	0.30	0.40	0.66	87	0.31	110
AAE	9.029	38.766	2442	909	17	0.53	0.46	2.46	0.30	194	0.24	43
AAI	-3.700	128.167	80	189	8	0.71		0.23				
AAM	42.300	-83.656	254	382	13	0.53	0.45	0.52	0.39	36		
ABQ	34.943	-106.458	1849	311	10	0.39	0.29	0.20	0.35	70		
ABU	34.859	135.573	200	781	14	0.53	0.41	0.51	0.48	157	0.39	94
ACO	36.699	-99.146	521	63	3	0.10		-0.38				
AD-	51.875	-176.679	61	54	5	0.14		0.65				
ADE	-34.967	138.709	655	2499	17	0.44	0.36	0.38	0.36	122	0.07	94
ADK	51.884	-176.685	116	1244	14	0.84	0.51	-0.12	0.71	280	0.48	1
AFI	-13.910	-171.777	706	897	14	0.64	0.41	0.66	0.48	310	0.40	131
AFR	-17.538	-149.778	50	477	15	0.74	0.52	1.00	0.71	322	0.58	95
AGM	47.082	-69.023	238	153	10	0.78	0.48	0.64	0.95	141		
AIA	-65.250	-64.267	11	173	8	0.44		0.16				
AKU	65.687	-18.107	24	1026	17	0.33	0.29	1.68	0.22	164	0.14	135
ALA	37.242	-115.115	0	47	3	0.25		0.28				
ALB	49.271	-124.822	25	210	9	0.39	0.34	0.90	0.28	276		
ALE	82.483	-62.400	65	3807	18	0.56	0.31	-0.52	0.61	42	0.22	108
ALG	36.772	3.058	59	176	11	0.76	0.70	-0.06	0.40	96		
ALI	38.355	-0.487	35	338	15	0.59	0.52	0.87	0.43	1	0.17	90
ALM	36.853	-2.460	65	239	12	0.61	0.57	0.69	0.39	154		
ALQ	34.942	-106.458	1853	2574	15	0.32	0.21	0.13	0.34	52	0.18	120
ALT	39.055	30.111	1060	220	8	0.28		0.22				
AMN	-17.851	-140.859	2	53	3	0.74		0.66				
ANG	17.155	-61.830	23	78	6	0.74		0.61				
ANK	39.917	32.817	0	381	12	0.53	0.52	0.65	0.15	16		
ANM	64.566	-165.372	330	36	4	0.85		0.92				
ANP	25.183	121.517	827	821	14	0.77	0.39	2.18	0.99	279	0.05	141
ANR	40.755	72.360	494	1864	17	0.39	0.37	0.79	0.18	313	0.09	108
ANT	-23.699	-70.415	80	282	16	0.72	0.53	0.08	0.32	44	0.69	104
ANV	64.566	-165.372	330	143	6	0.48		0.80				
APA	67.550	33.333	140	2460	18	0.55	0.39	0.41	0.57	232	0.16	69
APE	37.069	25.531	620	63	4	0.51		0.18				
APP	60.541	13.929	354	152	11	0.42	0.29	0.01	0.60	221		
APT	41.316	-72.064	3	196	11	0.58	0.55	0.98	0.30	131		
AQU	42.354	13.403	720	586	16	0.63	0.51	0.41	0.56	35	0.19	106
ARC	40.877	-124.075	59	73	5	0.37		1.75				
ARE	-16.462	-71.491	2452	688	18	0.74	0.43	-0.31	0.51	243	0.61	127
ARG	36.216	28.126	170	458	13	0.74	0.51	0.32	0.94	155		
ARH	45.010	1.312	320	531	15	0.32	0.31	0.62	0.11	52	0.05	135
ARN	37.349	-121.533	628	333	10	0.35	0.32	0.93	0.18	87		
ARO	11.529	42.847	680	41	5	0.40		1.56				
ARR	45.368	24.634	868	71	5	0.52		0.27				
ART	11.521	42.838	710	99	6	0.50		1.64				
ARU	56.400	58.600	250	662	14	0.41	0.32	-0.18	0.41	203	0.12	40
ASH	37.950	58.350	220	1587	17	0.42	0.28	0.95	0.41	22	0.25	96
ASP	-23.683	133.897	600	2512	16	0.47	0.40	-0.88	0.29	280	0.14	152
ASU	33.417	-111.933	354	88	6	0.35		1.01				
ATA	11.457	43.208	50	42	3	0.62		1.80				
ATH	37.972	23.717	95	1216	17	0.85	0.55	0.33	0.70	222	0.42	112
ATL	33.433	-84.337	272	384	6	0.70	0.47	-0.01	0.87	78		
AVE	33.298	-7.413	230	1124	17	0.43	0.40	0.49	0.17	234	0.07	94
AVF	46.791	3.353	225	324	12	0.36	0.32	-0.32	0.27	338		
AVY	-18.920	47.731	1716	236	8	0.68		0.72				
BAA	-34.592	-58.483	25	101	5	1.04		1.13				
BAB	30.121	-2.186	0	411	16	0.42	0.33	-0.23	0.29	205	0.27	118
BAC	46.567	26.900	168	469	13	0.79	0.75	0.70	0.34	75		
BAE	-15.841	-47.820	1200	198	11	0.77	0.22	-0.13	1.08	68		
BAF	47.835	6.995	1025	661	15	0.39	0.22	-0.25	0.42	322	0.17	162
BAG	16.411	120.580	1507	2286	16	0.69	0.30	-0.33	0.57	297	0.59	94
BAK	40.383	49.900	-12	430	11	0.58	0.52	3.52	0.47	208		
BAN	51.172	-115.558	1400	166	9	0.61	0.49	-0.88	0.45	342		
BAO	-15.635	-47.991	1211	324	16	0.62	0.34	-0.39	0.45	99	0.48	13
BAS	47.540	7.583	309	337	9	0.66	0.61	0.47	0.39	102		
BCK	37.460	30.589	860	309	9	0.39	0.33	0.42	0.35	272		
BCN	35.981	-114.834	776	1068	14	0.33	0.21	0.97	0.35	47	0.18	3
BCR	7.019	-73.176	750	170	13	1.08	0.81	-0.77	0.93	2		
BCT	41.493	-73.384	69	197	11	0.41	0.35	0.60	0.33	129		
BDB	43.065	0.148	561	286	11	0.48	0.46	-0.08	0.31	353		
BDF	-15.664	-47.903	1260	174	12	0.56	0.50	-0.41	0.32	94		
BDT	17.233	99.050	0	139	6	0.81		0.51				
BDW	42.776	-109.568	2190	373	12	0.33	0.30	-0.56	0.21	23		
BEC	32.379	-64.681	41	145	8	0.77	0.52	0.78	0.82	116		
BEI	42.117	-111.782	1859	230	12	0.42	0.26	0.44	0.46	356		
BEL	51.833	20.817	180									
BEO	44.821	20.455	129	617	15	0.57	0.38	0.82	0.54	304	0.46	81
BER	60.387	5.326	22	1625	16	0.41	0.37	0.75	0.13	252	0.20	148
BES	47.250	5.987	311	596	13	0.38	0.35	0.26	0.22	302		
BFD	-37.176	142.544	235	1290	16	0.40	0.32	-0.09	0.12	48	0.31	77
BFW	46.487	-123.215	902	178	9	0.53	0.22	0.65	0.66	331		
BGO	41.378	-83.659	212	149	6	0.50		0.07				
BGV	21.294	106.229	15	94	6	0.84		1.79				
BHA	-14.447	28.468	1206	1120	17	0.74	0.59	-0.28	0.70	333	0.28	77
BHG	47.721	12.879	475	320	11	0.59	0.25	0.12	0.95	1		

TABLE 2. (continued)

CODE	LAT	LONG	ELEV	P-WAVE STATION CORRECTION NOBS	NW	RMS0	RMS1	A0	A1	E1	A2	E2
BHK	31.417	76.417	410	205	7	0.22		0.42				
BHP	8.961	-79.558	36	135	8	0.80	0.58	0.15	0.86	86		
BI2	69.623	-145.895	1100	209	10	0.39	0.23	0.08	0.56	353		
BIG	59.390	-155.217	562	384	12	0.57	0.41	0.25	0.58	338		
BIZ	45.939	26.104	410	131	7	2.32		-2.84				
BKR	41.733	43.517	1500	3285	17	0.35	0.19	0.96	0.41	93	0.12	152
BKS	37.877	-122.235	276	1881	17	0.48	0.33	1.19	0.40	56	0.36	15
BLA	37.211	-80.421	634	713	15	0.67	0.39	0.53	0.75	111	0.26	94
BLC	64.317	-96.017	16	2675	15	0.44	0.32	-1.00	0.39	36	0.17	70
BLF	-29.109	26.188	1420	348	14	0.46	0.33	0.36	0.32	118	0.41	164
BLO	39.172	-86.522	230	187	4	0.28		-0.86				
BLR	63.502	-145.845	792	833	15	0.51	0.39	0.06	0.37	104	0.20	41
BLY	44.749	17.184	256	44	4	0.55		0.09				
BME	30.916	-6.760	1078	182	10	0.44	0.43	0.56	0.23	140		
BMN	40.431	-117.222	1505	1085	15	0.46	0.31	0.34	0.49	5	0.25	149
BMO	44.849	-117.306	1189	2457	15	0.40	0.27	-0.50	0.30	298	0.29	134
BNG	4.435	18.547	378	1545	18	0.53	0.47	-0.67	0.28	193	0.19	104
BNH	44.591	-71.256	472	543	14	0.50	0.25	0.76	0.65	137	0.09	10
BNS	50.964	7.176	200	1838	17	0.29	0.22	0.55	0.01	135	0.26	120
BOD	57.850	114.183	250	3296	16	0.57	0.34	-0.67	0.76	144	0.12	107
BOG	4.623	-74.065	2658	668	16	0.60	0.32	1.21	0.66	252	0.32	13
BOK	23.783	85.883	298	338	10	0.46	0.30	0.76	0.45	103		
BOL	44.487	11.329	80	65	4	0.76		2.06				
BOM	18.900	72.817	0	445	10	0.73	0.37	0.74	1.10	200		
BOU	40.008	-105.271	1654	119	8	0.28		1.07				
BOZ	45.600	-111.633	1575	582	15	0.24	0.19	-0.16	0.21	8	0.10	108
BPT	41.222	-73.242	83	173	11	0.54	0.31	0.47	0.66	128		
BRA	48.168	17.105	270	1950	17	0.51	0.29	0.14	0.47	28	0.28	22
BRG	50.874	13.946	296	2078	16	0.13	0.12	0.12	0.04	284	0.09	63
BRK	37.873	-122.260	81	99	6	0.28		0.78				
BRL	52.464	13.301	50	66	4	0.31		1.59				
BRN	52.419	13.203	45	165	8	0.28		1.12				
BRS	-27.392	152.775	525	2815	17	0.46	0.40	-0.02	0.28	251	0.25	24
BRW	71.303	-156.748	0	1083	15	0.53	0.35	0.48	0.62	348	0.38	59
BSF	47.833	6.794	1200	1359	16	0.29	0.22	-0.11	0.22	338	0.14	2
BTR	-2.617	29.733	1648	73	7	0.45		0.73				
BTY	36.883	-116.767	1183	36	2	0.46		0.37				
BUB	47.749	8.603	740	314	10	0.73	0.43	-0.97	1.11	355		
BUC	44.414	26.097	82	809	14	0.69	0.48	0.85	0.78	153		
BUD	47.484	19.024	196	1189	15	0.57	0.44	1.02	0.46	22	0.26	153
BUH	48.676	8.228	750	1392	18	0.44	0.27	-0.22	0.43	337	0.20	164
BUL	-20.143	28.613	1341	2219	17	0.46	0.36	-0.40	0.20	37	0.33	138
BUT	46.013	-112.563	1758	973	16	0.40	0.34	0.30	0.28	60	0.13	137
BYI	-80.005	-119.043	1449	219	9	0.51	0.35	0.53	0.53	124		
BYA	-80.017	-119.517	1515	52	3	0.70		0.33				
BYR	-80.017	-119.517	1515	316	10	0.75	0.74	0.	0.24	173		
CAF	44.926	2.064	630	183	7	0.29		0.41				
CAL	22.535	88.367	6	190	9	0.55		3.30				
CAN	-35.321	148.999	700	2946	17	0.40	0.38	0.42	0.15	122	0.05	72
CAR	10.507	-66.927	1032	1029	16	0.49	0.30	-0.27	0.59	56	0.08	12
CBM	46.932	-68.121	250	494	14	0.32	0.20	0.30	0.29	145	0.19	48
CBZ	-52.560	169.159	30	48	4	0.45		1.97				
CDF	48.412	7.276	1100	1476	15	0.32	0.20	-0.03	0.32	342	0.14	15
CDR	43.675	5.767	368	403	12	0.40	0.37	0.25	0.27	324		
CED	34.277	-117.334	1067	92	5	0.34		0.91				
CEN	-31.576	-68.754	900	338	15	0.65	0.40	-0.24	0.60	348	0.47	83
CER	-33.362	19.295	472	130	9	0.88		1.43				
CFA	-31.607	-68.239	622	106	10	0.75	0.49	-0.33	0.77	333		
CFF	45.763	3.102	400	197	7	0.76		0.87				
CFR	45.185	28.153	0	87	4	0.27		-0.37				
CGM	37.317	-89.533	134	50	4	0.31		-0.52				
CHA	26.833	87.167	161	364	12	0.49	0.47	0.61	0.19	152		
CHC	35.917	-79.050	149	183	6	0.79		0.78				
CHG	18.790	98.977	416	2285	18	0.64	0.32	-0.30	0.71	137	0.31	122
CHI	41.900	-87.633	183	147	5	0.37		-0.72				
CHN	4.967	-75.617	1360	142	9	0.90	0.87	-0.28	0.33	117		
CHT	22.350	91.817	35	462	11	0.61	0.43	1.94	0.74	182		
CHZ	50.292	18.992	316	40	3	0.14		1.36				
CIN	37.600	28.087	0	1151	15	0.23	0.22	-0.15	0.09	153	0.14	11
CIR	-21.013	31.580	430	1314	16	0.53	0.40	0.14	0.26	81	0.44	166
CIZ	-43.955	-176.566	45	67	3	0.18		1.90				
CLC	35.817	-117.597	766	162	6	0.39		0.30				
CLE	41.489	-81.532	328	692	15	0.71	0.34	0.83	0.76	62	0.38	49
CLK	-15.680	34.977	781	1216	16	0.36	0.28	0.14	0.14	210	0.30	145
CLL	51.310	13.003	230	4210	17	0.27	0.23	0.	0.04	315	0.18	112
CLS	38.637	-122.585	457	67	2	0.41		0.71				
CMC	67.833	-115.083	31	947	15	0.61	0.40	-0.08	0.12	194	0.75	47
CMP	45.268	25.038	598	1628	17	0.68	0.26	1.03	0.96	8	0.04	13
CNG	-26.292	32.188	100	698	16	0.53	0.50	0.50	0.09	21	0.24	152
CNH	43.830	125.313	0	141	8	0.45		-0.02				
CNN	39.137	-84.277	203	164	5	0.31		-0.52				
CNT	23.092	113.338	9	94	5	0.28		1.32				
CNU	30.660	104.012	0	131	7	0.76		0.28				
CNZ	-39.200	175.547	1116	271	8	0.63		0.77				
COB	-41.088	172.734	213	858	12	0.58	0.42	0.31	0.55	352		

TABLE 2. (continued)

CODE	LAT	LONG	ELEV	P-WAVE STATION CORRECTION								
				NOBS	NW	RMSO	RMS1	A0	A1	E1	A2	E2
COI	40.207	-8.418	140	171	11	0.34	0.29	0.79	0.25	18		
COL	64.900	-147.793	320	4815	17	0.72	0.37	-0.39	0.82	6	0.21	155
COM	16.253	-92.128	1528	197	9	0.76	0.46	1.04	0.92	238		
CON	-36.828	-73.045	15	144	10	0.71	0.60	0.12	0.56	297		
COO	-30.578	151.892	653	563	12	0.45	0.30	0.73	0.48	278		
COP	55.683	12.433	13	1576	16	0.58	0.29	1.07	0.42	304	0.57	120
COR	44.586	-123.303	123	317	11	0.55	0.38	1.43	0.50	322		
CPO	35.595	-85.570	574	2088	15	0.73	0.32	-0.53	0.90	111	0.25	112
CPP	-27.354	-70.351	384	68	2	0.34		-0.20				
CPX	36.932	-116.055	1285	35	2	0.42		0.97				
CRC	37.242	-122.130	607	78	5	0.31		1.45				
CRO	34.150	-94.556	302	167	6	0.63		-0.49				
CRT	37.190	-3.598	774	396	15	0.45	0.36	1.27	0.36	232	0.10	132
CRZ	-34.432	172.680	140	211	6	0.46		1.38				
CSC	34.000	-81.033	94	249	7	0.79		-0.01				
CSSM	36.026	-117.767	1143	136	5	0.06		0.74				
CTA	-20.088	146.254	357	3222	16	0.51	0.36	-0.31	0.32	196	0.48	133
CUM	10.465	-64.169	34	182	10	0.87	0.83	1.19	0.33	178		
CVF	42.568	8.869	530	238	8	0.35		0.13				
CWF	52.738	-1.307	187	350	12	0.37	0.36	0.26	0.14	339		
CYA	-28.444	-65.794	567	68	5	0.62		-0.83				
DAC	36.277	-117.594	1433	321	13	0.47	0.42	0.85	0.29	70		
DAG	76.770	-18.770	16	1809	18	0.51	0.29	-0.53	0.56	159	0.29	158
DAL	32.846	-96.784	187	274	11	0.28	0.25	0.65	0.17	126		
DAR	-12.408	130.818	6	769	13	0.58	0.44	-0.47	0.21	223	0.42	80
DAV	7.088	125.575	85	1218	14	0.77	0.43	0.45	0.26	313	0.82	111
DBN	52.102	5.177	3	836	15	0.56	0.47	1.43	0.19	115	0.47	151
DBQ	42.507	-90.683	244	327	6	0.45		-0.35				
DCC	-10.510	25.455	1425	55	5	0.45		0.67				
DCI	43.955	-111.096	2020	92	3	0.57		0.60				
DCN	53.343	-7.278	150	161	8	0.29		0.29				
DCU	40.414	-111.527	1829	99	6	0.41		0.84				
DDI	30.322	78.056	682	1086	15	0.54	0.43	0.29	0.43	330	0.20	126
DDK	53.387	-6.339	85	120	6	0.28		0.34				
DDR	35.998	139.193	800	2194	14	0.48	0.35	0.12	0.42	78	0.46	100
DEL	56.470	13.870	150	31	2	0.50		0.21				
DEV	45.903	22.900	250	1009	15	0.54	0.44	0.59	0.39	27	0.31	61
DIM	42.050	25.583	0	77	4	0.58		0.96				
DIX	46.080	7.411	2400	381	14	0.62	0.32	-0.61	0.59	287	0.35	22
DJA	-6.183	106.833	8	192	7	0.47		1.18				
DMK	41.822	27.757	280	633	12	0.39	0.38	0.18	0.13	274		
DMU	53.899	-6.911	280	33	2	0.07		-0.08				
DNP	-8.650	115.217	15	231	9	0.79		0.37				
DNY	42.836	-78.169	381	44	2	0.34		-0.32				
DOM	15.296	-61.391	15	52	6	0.30		0.12				
DON	37.176	-89.933	165	58	4	0.40		-0.93				
DOU	50.096	4.594	225	2556	17	0.41	0.33	0.69	0.28	23	0.23	115
DRB	39.581	28.637	620	198	8	0.43		-0.14				
DRV	-66.665	140.009	40	996	15	0.67	0.41	0.05	0.80	90	0.16	69
DSH	38.558	68.775	847	3128	18	0.57	0.35	0.74	0.64	255	0.23	73
DST	39.605	28.628	685	213	7	0.35		-0.49				
DUG	40.195	-112.813	1477	2910	16	0.35	0.16	0.22	0.26	54	0.37	152
DUN	-7.409	20.837	709	86	7	0.49		-0.58				
DUR	54.767	-1.583	103	902	16	0.75	0.63	1.19	0.23	317	0.52	122
EAB	56.188	-4.340	250	743	15	0.39	0.27	0.15	0.47	320	0.03	54
EAU	55.844	-3.455	350	700	15	0.42	0.33	0.28	0.14	17	0.33	159
EBH	56.248	-3.508	375	829	16	0.41	0.38	0.13	.10	315	0.16	178
EBL	55.773	-3.044	365	704	16	0.45	0.34	0.20	0.22	39	0.38	160
EBR	40.821	0.493	50	642	15	0.53	0.41	1.30	0.32	158	0.59	145
EBS	45.000	-101.232	735	60	3	0.19		0.13				
ECH	48.216	7.158	580	365	14	0.42	0.21	-0.58	0.63	353		
ECT	41.835	-73.411	342	168	10	0.44	0.37	0.89	0.40	112		
EDC	40.347	27.864	270	330	9	0.23		0.32				
EDI	55.923	-3.186	125	516	14	0.46	0.37	0.12	0.20	57	0.33	167
EDM	53.222	-113.350	730	3336	16	0.52	0.22	-0.63	0.64	4	0.17	133
EDU	56.547	-3.014	275	684	14	0.30	0.25	0.05	0.21	357	0.12	175
EGL	55.862	-2.738	245	866	16	0.31	0.21	0.22	0.10	61	0.32	173
EIL	29.550	34.950	200	1792	18	0.83	0.29	0.30	1.16	181		
EKA	55.333	-3.159	300	2675	18	0.34	0.28	0.18	0.16	7	0.19	163
ELC	37.285	-89.227	153	248	9	0.49	0.44	-0.75	0.25	339		
ELK	40.745	-115.239	2210	60	4	0.42		0.64				
ELL	36.749	29.908	1230	620	13	0.62	0.40	0.61	0.48	204	0.58	168
ELO	56.471	-3.706	495	379	13	0.44	0.33	-0.10	0.58	337		
ELT	53.250	86.267	0	3152	18	0.41	0.34	-0.62	0.13	231	0.32	159
ELY	39.131	-114.892	2011	43	3	0.15		0.69				
EMM	44.739	-67.489	20	336	11	0.50	0.32	0.59	0.67	134		
EPF	43.031	0.340	750	136	8	0.49		0.05				
ERB	-4.193	152.162	180	45	3	0.71		0.68				
ERE	40.183	44.500	990	280	9	0.31	0.25	1.04	0.28	337		
ERZ	39.915	41.277	1850	463	13	0.52	0.47	0.64	0.37	9		
ESA	-9.738	150.814	46	942	15	0.37	0.32	0.26	0.28	207	0.09	148
ESK	55.317	-3.205	242	1569	17	0.27	0.26	0.26	0.13	13	0.08	97
ESM	-4.277	152.686	50	67	7	0.94		-0.55				
ETV	-4.229	151.676	140	65	4	0.78		0.02				
EUR	39.483	-115.970	2178	3334	16	0.35	0.23	0.44	0.23	52	0.30	170

TABLE 2. (continued)

CODE	LAT	LONG	ELEV	P-WAVE STATION CORRECTION								
				NOBS	NW	RMSO	RMS1	A0	A1	E1	A2	E2
EWT	-4.115	152.087	30	63	5	0.95		0.27				
EZN	39.827	26.322	86	464	13	0.44	0.43	-0.26	0.17	173		
FAV	36.121	-94.190	387	991	14	0.40	0.29	-0.93	0.34	150	0.09	106
FAY	36.091	-94.191	404	431	9	0.57		-0.50				
FBA	64.900	-147.793	320	123	8	0.86		-0.16				
FBC	63.733	-68.467	45	1790	17	0.52	0.35	-0.53	0.46	141	0.26	78
FCC	58.762	-94.087	39	1996	16	0.48	0.31	-0.54	0.50	35	0.04	38
FDF	14.733	-61.156	510	111	6	0.55		0.06				
FEA	39.619	-121.246	1227	76	6	0.30		0.				
FEL	47.875	8.017	1485	92	5	0.57		-0.43				
FFC	54.725	-101.978	338	2923	14	0.44	0.35	-0.83	0.36	36	0.08	70
FGU	40.926	-109.386	1982	608	15	0.48	0.37	-0.29	0.38	39	0.18	146
FHC	40.802	-123.985	610	959	16	0.28	0.22	0.98	0.18	341	0.18	148
FIR	43.774	11.255	40	503	13	0.54	0.44	0.87	0.57	329		
FLG	35.293	-111.702	2445	112	6	0.37		1.57				
FLN	48.762	-0.482	230	2361	16	0.43	0.27	0.04	0.50	292	0.09	80
FLO	38.802	-90.370	160	456	11	0.37	0.31	-0.56	0.31	97		
FLR	41.717	-71.122	52	51	2	0.80		1.42				
FOC	45.695	27.183	61	331	9	0.88	0.57	1.02	1.05	128		
FOR	40.863	-73.886	24	74	3	0.34		0.67				
FRB	63.747	-68.547	18	1071	17	0.33	0.23	-0.46	0.23	75	0.27	84
FRE	36.767	-119.797	88	127	5	0.38		0.72				
FRI	36.992	-119.708	119	1316	16	0.53	0.17	0.12	0.66	343	0.20	7
FRM	37.836	-90.486	161	42	3	0.79		0.24				
FRR	-18.717	47.599	1554	270	9	0.80	0.37	1.01	1.16	272		
FRT	-18.170	-141.042	2	40	3	0.97		0.88				
FRU	42.833	74.617	655	3422	18	0.34	0.26	0.86	0.26	268	0.12	125
FRZ	42.281	20.038	0	55	3	0.39		0.53				
FSJ	54.433	-124.250	772	2122	16	0.55	0.39	0.70	0.50	170	0.43	176
FUQ	5.470	-73.738	2580	103	5	0.72		-0.27				
FUR	48.166	11.276	565	2362	16	0.41	0.28	0.33	0.49	349	0.09	119
FVM	37.983	-90.426	305	425	14	0.52	0.34	-0.49	0.40	133	0.29	36
FYU	66.566	-145.231	137	1059	16	0.58	0.33	0.58	0.50	344	0.35	168
GAP	47.477	11.064	725	239	9	0.47		0.25				
GAR	39.000	70.317	1300	2906	17	0.55	0.35	-0.25	0.51	318	0.41	97
GBA	13.604	77.436	25	2855	17	0.39	0.31	0.10	0.17	130	0.31	109
GBV	38.430	-79.844	826	47	4	0.74		0.80				
GCA	36.974	-111.593	1339	778	16	0.57	0.30	0.96	0.61	159	0.17	108
GDH	69.250	-53.533	23	1895	18	0.57	0.44	0.21	0.16	14	0.49	108
GEN	44.418	8.930	53	82	5	0.56		-0.46				
GEO	38.900	-77.067	43	171	7	0.35		0.44				
GIB	37.983	14.017	990	90	9	1.38	0.45	0.91	2.24	181		
GIL	64.975	-147.495	350	3542	16	0.71	0.40	-0.47	0.77	14	0.32	148
GIP	50.592	5.974	0	146	9	0.63		0.96				
GLA	33.052	-114.827	627	761	15	0.28	0.17	0.87	0.29	86	0.16	22
GLD	39.751	-105.221	1762	209	8	0.62		1.24				
GLP	40.287	30.310	560	540	14	0.74	0.45	-0.41	0.50	109	0.88	7
GLS	-25.035	128.296	600	410	10	0.54	0.31	-0.43	0.71	253		
GMA	65.429	-161.232	858	2237	16	0.39	0.31	-0.03	0.37	334	0.14	70
GMW	47.548	-122.786	506	249	10	0.59	0.26	0.63	0.72	346		
GNZ	-38.644	178.022	30	777	11	0.96	0.40	0.88	1.02	138		
GOA	15.483	73.817	58	205	7	0.83		0.44				
GOL	39.700	-105.371	2359	2014	15	0.28	0.19	0.29	0.18	331	0.24	125
GOT	57.698	11.978	66	414	9	0.49	0.34	-0.24	0.62	267		
GPA	40.287	30.310	560	260	9	0.51	0.42	-0.03	0.47	314		
GPD	41.018	-74.461	360	71	5	0.70		0.27				
GRC	47.296	3.074	191	983	15	0.24	0.20	0.05	0.08	30	0.12	173
GRE	12.047	-61.746	15	132	6	0.72		0.88				
GRF	49.692	11.215	525	2693	16	0.42	0.23	0.22	0.59	6	0.08	90
GRM	-33.313	26.573	610	280	13	0.77	0.68	0.39	0.50	47		
GRR	48.388	-0.858	220	2487	17	0.49	0.35	0.16	0.47	271	0.07	157
GRS	39.500	46.333	1550	2863	17	0.46	0.37	0.25	0.39	59	0.26	134
GRV	37.053	-90.395	168	36	3	0.19		-0.81				
GSC	35.302	-116.805	989	332	11	0.62	0.37	0.72	0.81	63		
GSP	-44.134	170.018	840	312	10	0.47	0.45	0.60	0.20	70		
GUA	13.538	144.912	230	605	13	0.86	0.75	-0.49	0.59	189		
GUMO	13.588	144.866	14	201	10	0.99	0.70	-0.16	1.04	248		
GWC	55.292	-77.753	8	1104	18	0.48	0.35	-0.61	0.34	43	0.28	60
GZR	45.393	22.777	850	64	4	0.29		0.05				
HAD	31.995	-4.455	1124	127	5	0.88		1.14				
HAL	44.633	-63.600	56	455	15	0.63	0.43	0.26	0.39	246	0.53	34
HAM	53.465	9.925	30	210	10	0.36	0.32	1.22	0.27	62		
HAN	46.603	-119.467	329	43	4	0.85		0.18				
HAU	48.005	6.350	570	1410	16	0.35	0.21	-0.07	0.26	320	0.26	16
HBF	32.933	-80.377	12	37	3	0.74		-0.03				
HBM	39.402	-120.153	1804	53	2	0.07		1.39				
HCC	36.981	-121.722	159	39	3	0.32		1.98				
HDM	41.486	-72.523	24	220	11	0.74	0.66	0.79	0.54	113		
HEE	50.883	5.983	100	982	16	0.43	0.35	0.87	0.35	137	0.28	151
HEI	49.399	8.726	560	46	4	0.42		0.19				
HEN	22.000	120.750	22	68	4	1.13		2.43				
HFS	60.134	13.696	265	2730	17	0.43	0.33	-0.62	0.19	261	0.35	96
HHM	48.349	-114.027	1100	1303	15	0.29	0.22	-0.38	0.12	284	0.21	138
HKC	22.304	114.172	27	1619	16	0.50	0.41	1.41	0.28	182	0.36	86
HKL	20.728	-156.255	0	43	3	0.50		2.07				

TABLE 2. (continued)

CODE	LAT	LONG	ELEV	P-WAVE STATION CORRECTION								
				NOBS	NW	RMS0	RMS1	A0	A1	E1	A2	E2
HKT	29.950	-95.833	-122	416	13	0.48	0.46	0.38	0.20	246		
HLE	51.500	11.950	92	197	8	0.24		-0.20				
HLG	54.185	7.884	41	95	6	0.41		1.59				
HLW	29.858	31.342	116	824	18	0.54	0.33	0.63	0.55	218	0.29	179
HNH	43.705	-72.286	180	57	4	0.60		1.15				
HNR	-9.432	159.947	72	997	13	0.48	0.46	0.21	0.18	317		
HOF	50.314	11.877	566	344	13	0.46	0.42	0.39	0.31	161		
HON	21.322	-158.008	2	607	12	0.59	0.49	1.66	0.48	231		
HSS	42.965	141.232	215	210	11	0.91	0.48	0.72	1.16	208		
HUA	-12.038	-75.323	3313	723	18	0.63	0.45	0.85	0.53	230	0.35	152
HVD	-30.604	25.496	1378	273	14	0.48	0.42	0.37	0.34	130	0.22	4
HVO	19.423	-155.293	1240	515	12	0.70	0.48	0.91	0.69	239		
HWA	23.967	121.617	18	123	5	0.58		2.69				
HYB	17.417	78.553	510	2699	17	0.34	0.29	-0.25	0.22	175	0.13	101
IAS	47.193	27.562	160	931	13	0.52	0.49	0.02	0.27	94		
IFR	33.517	-5.127	1630	1538	18	0.58	0.33	0.45	0.64	155	0.34	114
ILG	77.947	-39.183	2401	164	9	0.36	0.33	-0.61	0.27	253		
ILT	67.900	-178.700	0	3009	16	0.35	0.26	-0.04	0.20	6	0.25	157
IMA	66.068	-153.678	1380	1156	16	0.38	0.21	-0.36	0.45	331	0.30	39
INH	-19.547	169.273	110	96	5	0.58		0.18				
INK	68.292	-133.500	46	2883	17	0.36	0.27	-0.52	0.20	323	0.24	152
INY	42.444	-76.483	238	69	5	0.75		0.41				
IR1	35.416	50.689	1347	228	6	0.24		0.75				
IR7	35.703	50.609	1305	224	9	0.45		0.38				
IRK	52.272	104.310	467	2664	17	0.51	0.32	0.09	0.54	225	0.09	72
ISA	35.663	-118.473	835	131	7	0.80	0.46	0.86	0.92	51		
ISK	41.066	29.059	132	1202	17	0.44	0.33	-0.27	0.39	24	0.12	7
ISO	44.183	7.050	876	1384	16	0.42	0.32	0.16	0.19	305	0.33	149
IST	41.046	28.996	50	1298	17	0.66	0.55	0.46	0.44	122	0.35	173
ITM	37.180	21.927	400	145	8	0.82		-0.59				
IZM	38.398	27.262	630	517	14	0.50	0.35	0.07	0.52	177	0.13	124
JAN	39.657	20.851	540	547	15	0.55	0.44	0.41	0.55	195	0.24	172
JAS	37.947	-120.438	457	3207	16	0.31	0.16	0.30	0.39	19	0.19	137
JAY	-2.500	140.667	400	396	13	0.74	0.61	0.32	0.52	334		
JCT	30.479	-99.802	591	712	14	0.36	0.32	-0.48	0.09	139	0.23	1
JEN	50.952	11.583	193	269	7	0.71		0.19				
JER	31.772	35.197	770	1576	17	0.53	0.41	1.02	0.47	193	.10	102
JMI	70.927	-8.726	50	58	5	0.33		2.10				
JOS	48.496	20.539	280	1255	15	0.42	0.29	0.16	0.54	0	0.28	95
KAA	-20.777	116.859	15	137	5	0.93		-0.14				
KAD	17.305	74.183	581	38	4	0.42		-0.71				
KAR	24.933	67.143	34	520	11	0.79	0.69	1.41	0.70	210		
KAS	41.372	33.767	850	1740	17	0.41	0.30	0.56	0.24	73	0.28	8
KAT	39.200	56.267	90	1898	17	1.23	0.46	1.48	1.70	351	0.37	106
KBL	34.541	69.043	1920	2183	17	0.57	0.34	-0.19	0.39	234	0.43	120
KBS	78.917	11.924	46	2108	18	0.50	0.33	0.99	0.55	238	0.02	58
KCH	-49.244	70.145	0	49	4	0.51		2.23				
KDC	57.748	-152.492	0	2320	16	0.32	0.24	0.05	0.16	50	0.23	5
KDS	12.569	-12.211	110	122	8	0.80		-0.55				
KDZ	41.641	25.350	329	569	14	0.61	0.51	0.13	0.53	166	0.30	35
KEB	38.798	38.728	739	127	6	0.32		0.90				
KED	12.926	-12.321	0	159	8	1.42	0.28	-0.87	2.60	335		
KER	34.352	47.106	1310	1034	16	0.57	0.40	0.30	0.39	243	0.52	42
KES	31.995	-4.455	1124	354	15	0.46	0.42	0.71	0.23	200	0.10	174
KET	-4.333	152.036	17	60	5	0.74		0.56				
KEV	69.755	27.007	80	3938	18	0.35	0.30	0.34	0.22	198	0.09	167
KEW	51.468	-0.313	5	360	9	0.31	0.26	0.36	0.29	126		
KFC	37.956	-122.549	6	35	2	0.22		0.98				
KGM	2.017	103.318	103	221	8	0.43		0.63				
KHC	49.131	13.579	700	4113	17	0.52	0.23	-0.29	0.65	7	0.16	19
KHE	80.617	58.050	100	2761	18	0.67	0.34	0.94	0.80	239	0.12	7
KHI	34.143	58.642	1600	402	11	0.44	0.37	0.47	0.35	338		
KHO	37.483	71.533	1850	3076	18	0.56	0.34	0.52	0.53	307	0.37	114
KIC	6.361	-4.741	175	1347	18	0.53	0.39	-0.54	0.54	144	0.11	95
KIM	-28.752	24.780	1321	452	16	0.60	0.50	-0.34	0.22	93	0.43	150
KIP	21.423	-158.015	70	898	12	0.50	0.34	1.29	0.55	221		
KIR	67.840	20.417	390	4485	18	0.35	0.31	-0.18	0.21	262	0.06	64
KIS	47.017	28.867	49	1496	17	0.59	0.28	-0.54	0.72	98	0.12	12
KJF	64.199	27.715	160	2832	18	0.33	0.24	-0.12	0.31	324	0.11	82
KJN	64.085	27.712	250	2232	18	0.37	0.34	-0.22	0.17	320	0.04	90
KKI	-4.588	145.954	460	32	2	1.24		-0.80				
KKM	6.045	116.211	830	95	5	0.69		0.93				
KKR	29.963	76.825	257	184	8	0.77		1.79				
KKS	42.008	20.411	0	79	6	0.78		0.22				
KLG	-30.784	121.458	350	1885	17	0.28	0.22	-0.75	0.20	189	0.09	36
KLS	56.165	15.592	11	428	10	0.45	0.26	-0.40	0.80	232		
KMA	42.262	20.243	0	71	4	0.51		0.22				
KMR	48.057	14.132	379	90	7	0.66		0.62				
KMU	42.237	142.967	180	629	14	0.70	0.42	0.58	0.86	157	0.49	115
KNA	-15.750	128.767	55	1014	13	0.49	0.45	-0.62	0.30	96		
KNB	37.017	-112.822	1715	112	7	0.38		1.27				
KOA	-6.224	155.619	65	215	9	0.38	0.29	-0.71	0.41	64		
KOD	10.233	77.467	2343	2665	16	0.54	0.31	0.89	0.61	185	0.08	105
KON	59.649	9.598	200	2685	17	0.34	0.24	0.33	0.28	276	0.17	132
KOU	-20.562	164.281	17	1059	15	0.72	0.30	0.52	0.96	14	0.43	69

TABLE 2. (continued)

CODE	LAT	LONG	ELEV	P-WAVE STATION CORRECTION								
				NOBS	NW	RMS0	RMS1	A0	A1	E1	A2	E2
KPB	-49.520	69.901	0	48	4	0.85		2.12				
KPD	-49.517	70.157	0	52	5	0.80		2.14				
KPH	21.576	-158.275	0	66	5	0.42		0.79				
KPK	39.583	-121.305	899	501	13	0.15	0.14	0.44	0.12	200		
KRA	50.058	19.940	223	3340	17	0.24	0.18	0.10	0.23	358	0.08	65
KRK	69.724	30.062	0	865	17	0.33	0.30	0.45	0.14	111	0.16	173
KRL	49.011	8.412	114	683	15	0.52	0.41	1.12	0.57	1	0.26	113
KRP	-37.925	175.537	64	2162	14	0.78	0.46	0.41	0.40	315	0.65	89
KRR	-16.852	29.618	1380	1297	16	0.62	0.44	-0.22	0.17	144	0.68	163
KRT	-4.353	152.052	20	55	4	0.88		0.95				
KRV	40.650	46.333	340	2733	17	0.33	0.29	-0.32	0.13	81	0.22	122
KSA	33.824	35.892	923	1569	17	0.79	0.48	1.31	0.78	160	0.35	95
KSR	-25.850	26.897	1623	362	14	0.72	0.71	0.34	0.17	163		
KSU	11.517	42.446	370	53	5	0.55		1.59				
KT4	31.910	-103.315	948	59	4	0.36		0.18				
KT7	31.709	-103.306	847	44	2	0.03		0.54				
KTG	70.417	-21.983	6	2671	18	0.50	0.25	0.88	0.58	125	0.16	107
KUG	-10.183	123.667	52	237	11	1.58	0.73	1.35	1.84	138		
KUL	37.900	69.750	605	991	16	0.67	0.46	0.16	0.73	300	0.22	55
KUN	25.123	102.740	1922	161	6	0.69		0.44				
KUR	45.233	147.867	0	724	13	0.95	0.72	0.55	0.98	206		
KVT	41.081	36.046	650	398	8	0.48		0.61				
KYS	35.198	140.148	180	630	14	0.97	0.50	1.21	1.21	81	0.14	139
KZN	40.307	21.771	900	297	13	0.53	0.47	0.28	0.34	298		
LAC	34.390	-116.411	792	80	6	0.68		1.17				
LAE	-6.673	146.913	50	41	4	0.52		1.29				
LAH	31.550	74.333	210	933	14	0.41	0.30	0.10	0.37	311	0.25	87
LAN	36.050	103.833	1506	191	7	0.63		0.87				
LAO	46.689	-106.222	744	1547	15	0.47	0.25	-0.28	0.51	8	0.17	40
LAR	41.314	-105.583	2400	438	11	0.36	0.36	0.01	0.09	21		
LAT	-6.712	146.990	37	825	14	0.43	0.20	0.34	0.46	182	0.32	136
LAW	38.959	-95.250	0	422	11	0.36	0.36	-0.29	0.02	153		
LBF	46.987	3.977	660	1755	17	0.34	0.25	-0.01	0.20	221	0.26	165
LCG	21.145	-101.725	2200	259	13	0.50	0.42	1.77	0.38	110		
LD1	46.840	-105.889	759	357	12	0.55	0.23	0.15	0.75	32		
LD3	46.550	-106.480	801	87	5	0.38		-0.07				
LD4	46.942	-106.383	714	63	4	0.37		0.54				
LDM	48.454	-115.317	838	249	10	0.41	0.29	0.30	0.44	274		
LEE	37.243	-113.377	1067	98	3	0.18		1.19				
LEM	-6.833	107.617	1252	1923	17	0.91	0.45	0.90	1.08	194	0.47	28
LEN	40.767	43.850	1522	276	10	0.62	0.29	2.94	0.91	219		
LF1	47.371	-105.187	740	76	5	0.34		0.37				
LF2	45.909	-105.486	754	55	4	0.54		-0.48				
LF4	47.411	-106.944	707	242	3	0.37		-0.22				
LFF	44.937	0.736	160	1189	16	0.22	0.20	0.52	0.03	162	0.15	2
LGN	10.145	-71.270	3	39	2	0.83		-0.49				
LGR	42.458	-2.503	446	50	5	0.14		1.65				
LHA	29.637	91.037	3630	198	7	0.14		0.88				
LHC	48.417	-89.267	196	951	14	0.54	0.41	-0.57	0.38	73	0.31	58
LHN	61.049	10.880	505	809	16	0.49	0.32	0.09	0.51	269	0.07	32
LHS	34.479	-80.808	120	81	5	0.34		-0.01				
LIC	6.224	-5.028	100	545	17	0.60	0.47	-0.58	0.50	171	0.30	67
LIS	38.716	-9.149	77	339	15	0.66	0.64	1.21	0.24	292		
LJU	46.043	14.533	396	2237	17	0.35	0.31	0.11	0.21	141	0.12	150
LMG	-8.908	148.150	1200	309	9	0.48	0.15	0.44	0.68	155		
LMP	-16.426	167.800	60	284	7	0.47		0.36				
LMR	43.333	6.509	200	871	14	0.48	0.36	0.27	0.39	289	0.19	153
LMT	-41.610	146.152	349	70	3	0.15		0.84				
LND	43.040	-81.183	246	236	7	0.38		-0.18				
LNM	21.117	-101.667	1800	37	4	1.10		1.10				
LNR	-15.852	168.160	8	298	7	0.49		0.23				
LNS	45.289	6.915	1480	1297	16	0.67	0.26	0.43	0.67	295	0.44	178
LNV	-33.956	-71.411	0	136	9	0.64		-0.65				
LOM	6.122	1.213	5	56	4	1.00		1.53				
LON	46.750	-121.810	854	1581	16	0.44	0.24	0.16	0.39	263	0.32	161
LOR	47.267	3.851	520	3150	17	0.39	0.25	-0.04	0.32	284	0.23	170
LOT	45.448	23.769	1240	109	6	0.32		-0.80				
LPA	-34.909	-57.932	14	288	15	0.76	0.47	0.32	0.88	67	0.13	74
LPB	-16.533	-68.098	3292	873	18	0.72	0.59	-0.21	.10	156	0.58	65
LPF	48.032	-1.042	170	1080	15	0.51	0.36	0.17	0.48	297	0.12	156
LPO	44.683	1.187	330	1077	15	0.23	0.18	0.50	0.03	45	0.19	2
LPS	14.292	-89.162	1000	1033	14	0.43	0.39	0.34	0.10	323	0.24	41
LRG	43.454	6.361	100	831	14	0.44	0.31	0.58	0.30	278	0.28	161
LSF	46.250	1.534	425	1285	16	0.29	0.25	0.26	0.20	217	0.17	157
LSM	36.739	-116.278	1146	278	12	0.49	0.31	0.73	0.53	134		
LUB	33.583	-101.867	980	906	14	0.33	0.24	0.15	0.17	357	0.28	22
LUG	-15.518	167.130	150	1094	12	0.95	0.50	-0.35	1.38	271		
LUX	49.600	6.133	0	428	13	0.61	0.59	2.14	0.25	69		
LVN	36.109	-115.140	610	46	3	0.45		2.13				
LVV	49.817	24.033	308	1143	15	0.34	0.30	0.37	0.24	0	0.23	100
LWI	-2.238	28.800	1748	994	18	0.56	0.47	0.75	0.45	138	0.09	74
MAG	59.550	150.800	80	1791	14	1.46	0.55	0.29	1.85	186	0.37	41
MAIO	36.308	59.472	1150	643	15	0.38	0.24	0.53	0.47	15	0.17	108
MAK	43.017	47.433	10	711	15	0.70	0.47	1.59	0.69	224	0.36	8
MAL	36.727	-4.411	60	270	13	0.72	0.50	0.40	0.67	255	0.02	45

TABLE 2. (continued)

CODE	LAT	LONG	ELEV	P-WAVE STATION CORRECTION								
				NOBS	NW	RMS0	RMS1	A0	A1	E1	A2	E2
MAN	14.662	121.077	70	558	8	0.79		1.07				
MAT	36.542	138.209	440	3849	16	0.54	0.44	-0.35	0.40	51	0.28	73
MAW	-67.603	62.875	6	2010	17	0.58	0.45	-0.04	0.48	319	0.28	137
MBC	76.242	-119.358	15	3916	17	0.40	0.28	-0.29	0.32	24	0.29	67
MBL	-21.160	119.833	200	273	9	0.45	0.34	-0.37	0.46	250		
MBO	14.391	-16.955	3	398	13	0.63	0.48	1.17	0.61	284		
MBT	-21.170	119.742	200	338	11	0.26	0.25	-0.53	0.06	301		
MCC	52.052	-118.585	578	387	13	0.55	0.29	0.78	0.53	275	0.40	23
MCK	63.732	-148.935	610	33	2	0.59		-1.88				
MCQ	-54.499	158.956	14	292	8	0.29	0.17	1.00	0.39	10		
MCV	36.634	-116.000	1158	38	4	0.26		0.83				
MCW	48.680	-122.832	693	116	7	0.55		0.56				
MDC	37.882	-121.914	1173	84	4	0.23		1.31				
MDR	13.000	80.183	15	537	12	0.56	0.51	1.11	0.37	182		
MDZ	-32.883	-68.850	826	447	16	0.57	0.36	0.14	0.54	2	0.51	80
MED	3.550	98.683	32	338	12	1.12	0.95	0.61	0.84	116		
MEK	-26.613	118.545	515	1538	17	0.25	0.22	-0.80	0.13	257	0.12	47
MEM	50.609	6.007	0	230	11	0.91	0.70	0.75	0.84	111		
MES	38.199	15.555	45	338	13	1.18	0.56	0.59	1.57	181		
MFF	46.601	-0.143	260	1171	15	0.37	0.26	0.30	0.27	297	0.21	0
MFP	3.342	8.661	1338	122	10	0.73	0.58	0.88	0.80	170		
MFS	36.117	-117.855	1524	134	8	0.21		0.71				
MFW	45.903	-118.406	384	150	5	0.49		0.59				
MGD	60.100	150.700	220	419	11	0.63	0.39	-0.05	0.70	310		
MGL	39.807	-121.557	975	61	3	0.74		-0.19				
MGN	40.925	32.181	750	446	9	0.53		1.12				
MHC	37.342	-121.642	1282	2241	17	0.36	0.25	0.81	0.33	61	0.23	22
MHI	36.300	59.495	1100	256	11	0.52	0.26	0.20	0.85	39		
MHK	39.187	-96.579	314	220	12	0.47	0.47	-0.49	0.11	22		
MHT	39.200	-96.581	200	366	8	0.31		-0.81				
MID	59.428	-146.339	37	60	5	0.33		1.46				
MIM	45.244	-69.040	140	428	15	0.38	0.26	0.50	0.24	171	0.28	41
MIN	40.345	-121.605	1495	2091	16	0.31	0.23	-0.07	0.20	349	0.18	0
MIR	-66.550	93.000	30	1600	17	0.47	0.34	-0.16	0.12	48	0.40	94
MIZ	39.134	141.136	63	201	11	1.03	1.01	2.01	0.33	194		
MJP	-43.991	170.459	960	67	3	0.21		0.03				
MJZ	-43.987	170.466	1000	1165	13	0.55	0.40	0.65	0.66	67		
MKS	-5.067	119.633	28	375	11	1.04	0.47	0.89	1.60	70		
MLR	45.492	25.944	1360	1162	17	0.50	0.29	0.46	0.52	42	0.41	140
MLS	42.958	1.083	450	241	10	0.60	0.46	0.43	0.50	244		
MMA	33.554	-111.958	426	283	11	0.33	0.30	0.93	0.19	328		
MNG	-40.619	175.482	396	1633	13	0.68	0.26	-0.12	0.80	125		
MNI	1.450	124.800	128	144	7	0.61		0.29				
MNL	33.147	73.750	436	439	10	0.64	0.32	1.03	0.85	341		
MNS	42.387	12.680	0	46	5	0.43		0.06				
MNT	45.502	-73.623	112	1540	18	0.57	0.26	0.17	0.70	107	0.18	25
MNV	38.433	-118.153	1507	1240	15	0.41	0.19	0.19	0.20	0	0.44	140
MNW	-45.780	167.619	155	683	11	0.67	0.57	0.55	0.61	248		
MNY	44.961	5.691	422	878	15	0.81	0.43	0.52	0.73	268	0.46	164
MOA	47.850	14.266	572	519	14	0.50	0.23	-0.51	0.69	23		
MOK	21.456	-157.737	0	78	6	0.74		0.65				
MOM	-2.042	147.402	10	306	9	0.56	0.50	0.60	0.47	196		
MOO	-42.442	147.190	325	444	8	0.46		1.20				
MOS	55.738	37.625	124	3060	17	0.38	0.32	0.18	.10	156	0.28	160
MOT	30.680	-104.008	2020	286	9	0.39	0.35	0.06	0.27	56		
MOX	50.646	11.616	454	4074	17	0.26	0.19	0.08	0.23	5	0.19	96
MOY	51.683	100.983	0	2461	18	0.59	0.34	0.71	0.65	279	0.24	163
MPP	7.897	126.018	1200	93	5	1.20		-0.98				
MRG	39.633	-79.954	282	752	16	0.47	0.26	1.12	0.53	98	0.09	72
MSA	36.859	-106.018	3322	40	2	0.51		0.86				
MSH	36.311	59.588	999	1233	15	0.40	0.31	1.14	0.34	341	0.15	66
MSI	38.203	15.556	60	52	4	1.00		0.51				
MSO	46.829	-113.941	1264	1089	16	0.28	0.16	-0.16	0.25	53	0.25	134
MSP	16.350	120.562	2250	38	2	0.22		0.23				
MSZ	-44.671	167.917	38	1199	13	0.57	0.29	0.71	0.43	310	0.54	33
MTD	-16.780	31.583	967	727	16	0.63	0.54	-0.24	0.18	171	0.46	147
MTE	40.403	-7.537	815	204	12	0.41	0.28	0.47	0.45	107		
MTN	-12.846	131.130	155	1430	14	0.56	0.42	-0.74	0.27	180	0.41	75
MUI	36.312	59.605	1000	128	6	0.23		1.11				
MUN	-31.978	116.208	253	2212	17	0.66	0.52	-0.38	0.36	267	0.53	65
MWC	34.223	-118.058	1730	56	3	0.14		-0.18				
MWI	16.713	-62.222	46	61	6	0.61		0.86				
MZF	46.216	2.584	480	319	11	0.31	0.30	0.09	0.14	330		
MZO	36.132	-95.300	181	96	5	0.33		-0.64				
NAH	26.217	127.683	11	45	4	1.28		2.95				
NAI	-1.274	36.804	1692	975	17	0.91	0.44	2.03	1.02	259	0.31	178
NAN	32.063	118.783	7	123	5	0.54		0.65				
NAO	60.824	10.832	379	1411	17	0.60	0.34	-0.77	0.69	246	0.11	82
NB2	61.040	11.215	717	420	14	0.43	0.33	-0.11	0.37	270		
NBO	61.031	10.777	529	73	6	0.35		-1.04				
NC3	61.262	11.414	366	73	5	0.21		-0.40				
NCE	-0.661	-78.497	3821	32	2	0.44		2.55				
NDF	-17.757	177.450	30	261	7	1.08		1.99				
NDI	28.683	77.217	230	3934	18	0.57	0.44	-0.30	0.49	288	0.02	148
NEL	35.712	-114.844	1061	67	4	0.23		0.61				

TABLE 2. (continued)

CODE	LAT	LONG	ELEV	P-WAVE STATION CORRECTION								
				NOBS	NW	RMS0	RMS1	A0	A1	E1	A2	E2
NEM	43.328	145.587	26	129	8	0.96	0.31	-0.49	1.31	182		
NEW	48.263	-117.120	760	2936	15	0.39	0.22	-0.37	0.43	356	0.17	155
NGS	32.732	129.870	27	182	11	0.59	0.51	1.90	0.43	161		
NHA	12.210	109.212	5	234	5	0.24		0.22				
NIA	-29.042	167.960	130	63	3	0.59		1.72				
NIE	49.424	20.322	555	2679	17	0.35	0.31	0.55	0.13	356	0.22	74
NIK	52.974	-168.853	207	265	8	0.43		-0.69				
NIL	33.650	73.252	536	1928	18	0.47	0.33	-0.02	0.22	342	0.41	58
NKM	35.448	-5.410	158	270	12	0.69	0.46	1.05	0.67	270		
NLG	17.067	79.267	220	158	7	0.44		0.10				
NLM	39.032	-76.981	114	51	3	0.66		0.07				
NMC	35.844	-117.907	1080	42	3	0.29		1.07				
NNA	-11.988	-76.842	575	359	14	0.69	0.55	-0.20	0.12	261	0.52	149
NOR	81.600	-16.683	36	1893	18	0.46	0.39	-0.09	0.07	153	0.34	140
NOU	-22.310	166.451	105	1008	16	0.67	0.39	0.49	0.60	4	0.51	38
NP-	76.252	-119.372	59	703	14	0.34	0.19	0.21	0.26	88	0.31	45
NPA	-15.087	39.254	375	37	4	0.54		0.88				
NPL	40.847	14.258	7	76	7	0.52		0.88				
NPS	35.262	25.612	370	158	8	1.16	0.57	0.70	2.06	175		
NRA	63.889	-160.064	150	95	6	0.63		-0.20				
NRI	69.400	88.100	40	447	15	1.22	0.54	-0.28	1.63	284		
NRN	41.433	76.000	2849	742	15	0.44	0.22	0.09	0.51	2	0.27	112
NRR	39.572	-119.849	1650	278	10	0.30	0.24	0.24	0.27	33		
NTI	48.630	-116.963	823	1525	15	0.55	0.24	-0.19	0.68	355	0.18	145
NUE	-19.076	-169.928	56	54	3	0.13		1.32				
NUR	60.509	24.651	102	4579	18	0.21	0.17	-0.17	0.05	11	0.18	116
NVL	-70.767	11.833	87	704	14	0.72	0.44	0.10	0.86	2	0.28	109
NVS	54.900	83.300	0	426	11	0.38	0.35	-0.76	0.26	309		
NWA	-32.927	117.234	265	101	8	0.40		-0.22				
NWAO	-32.927	117.234	265	504	11	0.44	0.38	-0.47	0.35	93		
OAQ	-0.216	-78.499	2816	34	4	0.23		1.51				
OBN	55.167	36.600	0	2553	17	0.29	0.20	0.11	0.24	99	0.18	167
OBO	11.987	43.293	50	31	2	0.97		1.86				
OFD	36.067	1.600	377	49	3	0.45		0.53				
OGA	46.868	11.025	934	268	10	0.67	0.44	0.44	0.85	319		
OHC	-63.317	-57.900	20	48	4	0.81		-1.15				
OHR	41.111	20.799	739	915	17	0.66	0.40	-0.19	0.73	248	0.16	40
OIC	34.099	135.317	776	797	14	0.37	0.32	0.07	0.09	311	0.22	75
OIS	34.105	135.327	678	587	13	0.45	0.45	0.25	0.04	243		
OLC	38.040	-122.792	30	39	2	0.25		1.07				
OLO	36.457	-95.711	196	30	2	0.15		-0.84				
OPA	21.691	-158.012	150	132	7	0.79		1.29				
ORT	35.910	-84.305	370	687	14	0.75	0.35	0.50	0.75	123	0.33	76
ORV	39.555	-121.500	360	850	16	0.41	0.33	0.05	0.30	131	0.19	156
OTP	-18.168	-140.857	2	49	3	0.77		1.14				
OTT	45.394	-75.716	83	1589	18	0.59	0.39	0.06	0.52	99	0.35	66
OUA	-20.775	167.244	29	210	7	0.70		0.46				
OUL	65.085	25.896	60	1403	17	0.35	0.30	-0.51	0.15	318	0.22	89
OXM	19.297	-99.688	2700	214	10	0.99	0.80	0.81	0.80	114		
OYM	35.420	139.243	600	587	13	0.64	0.27	0.10	0.80	60	0.63	91
PAA	-6.301	155.491	699	298	10	0.46	0.30	-0.73	0.63	70		
PAD	45.409	11.886	12	136	8	0.68		3.07				
PAE	-17.662	-149.580	60	494	17	0.63	0.57	1.37	0.14	278	0.39	103
PAL	41.004	-73.909	91	479	14	0.56	0.40	0.11	0.52	113	0.33	128
PAO	40.598	110.018	0	164	9	0.43	0.41	0.96	0.16	292		
PAS	34.148	-118.172	295	2291	17	0.41	0.23	0.85	0.44	78	0.20	16
PAT	38.236	21.747	40	33	3	0.49		0.30				
PAV	45.183	9.174	77	151	8	1.12		0.67				
PBA	11.667	92.717	79	250	11	0.82	0.71	1.82	0.69	229		
PBJ	16.437	-95.407	213	169	8	0.78		0.19				
PCO	36.691	-96.978	331	46	2	0.28		-0.53				
PCT	14.715	101.427	0	77	5	0.66		0.48				
PDA	37.743	-25.662	35	143	9	0.37		1.72				
PEC	33.892	-117.161	616	105	6	0.84		0.83				
PEK	40.040	116.175	0	1256	16	0.55	0.52	0.27	0.17	204	0.19	108
PEL	-33.144	-70.685	690	380	15	0.33	0.22	-0.25	0.27	343	0.32	90
PET	53.017	158.650	25	1626	14	0.65	0.39	-0.06	0.31	220	0.72	26
PGC	48.650	-123.451	5	31	2	0.17		0.49				
PHC	50.707	-127.432	33	665	14	0.58	0.42	1.11	0.51	27	0.53	76
PHI	39.959	-75.175	5	41	3	0.49		2.75				
PI5	42.567	-109.912	2273									
PI6	42.726	-109.605	2225	117	6	0.83		-0.87				
PIM	18.275	-101.882	81	86	7	0.96		0.14				
PJD	65.035	-147.508	740	669	14	0.77	0.44	-0.17	0.92	8	0.21	134
PJG	13.588	144.866	14	160	10	1.11	0.99	-0.55	0.67	177		
PKR	-30.003	24.742	1267	180	11	0.60	0.59	0.67	0.18	77		
PLG	40.374	23.446	580	634	15	0.62	0.51	0.08	0.47	184	0.18	82
PLP	11.250	125.000	0	82	5	0.66		0.81				
PLV	20.806	106.629	90	320	9	0.80	0.25	2.60	1.17	174		
PMA	55.979	-160.497	314	64	6	0.35		0.54				
PMG	-9.409	147.154	70	2013	15	0.51	0.28	0.26	0.54	179	0.34	140
PMO	-15.004	-147.897	2	684	16	0.72	0.56	0.84	0.54	295	0.43	97
PMR	61.592	-149.131	0	3869	16	0.49	0.30	-0.44	0.62	40	0.09	65
PNI	44.919	7.314	585	33	5	0.76		-1.66				
PNJ	40.907	-74.155	31	64	5	0.48		0.91				

TABLE 2. (continued)

CODE	LAT	LONG	ELEV	P-WAVE STATION CORRECTION								
				NOBS	NW	RMS0	RMS1	A0	A1	E1	A2	E2
PNL	59.669	-139.397	579	83	6	0.65		0.63				
PNO	45.612	-118.763	402	50	3	0.40		0.31				
PNS	-16.267	-68.473	3986	580	18	0.58	0.42	-0.13	0.28	235	0.50	50
PNT	49.317	-119.617	550	2521	16	0.29	0.27	-0.11	0.15	48	0.09	162
POO	18.533	73.850	556	2385	15	0.43	0.33	0.05	0.35	270	0.15	117
POW	36.152	-91.185	156	203	8	0.53	0.36	-0.61	0.68	88		
PPI	-0.452	100.384	0	258	10	0.74	0.61	0.34	0.77	222		
PPN	-17.531	-149.432	100	649	17	0.76	0.63	1.27	0.52	314	0.48	95
PPT	-17.569	-149.576	260	760	17	0.67	0.56	1.35	0.45	331	0.45	94
PRA	50.070	14.433	225	1664	16	0.45	0.34	0.53	0.50	354	0.17	117
PRE	-25.753	28.190	1333	1484	16	0.55	0.26	-0.07	0.46	51	0.44	146
PRG	43.101	12.397	495	89	5	0.40		1.63				
PRI	36.142	-120.665	1187	2267	16	0.41	0.18	1.08	0.36	358	0.40	16
PRK	39.246	26.272	100	739	15	0.42	0.27	0.64	0.48	200	0.12	156
PRM	34.083	-82.363	254	149	8	0.52	0.29	-0.20	0.76	80		
PRS	36.332	-121.370	363	194	9	0.15		0.62				
PRT	43.883	11.092	62	200	7	0.48		1.74				
PRU	49.988	14.542	302	3929	17	0.52	0.29	0.07	0.69	3	0.33	95
PRY	-26.928	27.473	1445	272	13	0.56	0.49	-0.26	0.38	108		
PRZ	42.483	78.400	1599	1788	17	0.46	0.32	0.99	0.10	186	0.43	104
PSH	33.937	71.434	456	849	14	0.52	0.21	0.01	0.53	259	0.77	74
PSI	2.691	98.919	0	450	11	1.17	1.04	-0.12	1.06	204		
PSO	1.192	-77.325	3010	252	14	0.56	0.44	0.46	0.25	189	0.44	176
PSZ	47.919	19.894	940	654	14	0.52	0.39	-0.15	0.62	356	0.22	82
PTL	38.049	23.865	500	278	11	0.70	0.41	0.30	0.92	220		
PTN	44.572	-74.983	238	167	9	0.60	0.22	0.07	0.99	97		
PTO	41.139	-8.602	88	784	15	0.47	0.41	-0.07	0.30	62	0.13	67
PUK	42.043	19.893	0	55	3	0.32		0.62				
PUL	59.767	30.317	65	1861	16	0.47	0.46	0.31	0.05	191	0.13	94
PVC	-17.740	168.312	80	605	10	0.68	0.51	0.01	0.90	315		
PVL	43.147	25.172	187	676	15	0.46	0.39	0.57	0.25	133	0.20	57
PYA	44.033	43.058	497	1252	15	0.32	0.25	0.49	0.18	299	0.19	146
PYR	34.568	-118.741	1247	149	7	0.13		0.89				
QCP	14.637	121.077	58	536	9	0.48		1.25				
QMB	53.765	-1.858	116	125	8	0.38		0.39				
QUE	30.188	66.950	1721	3742	18	0.48	0.30	0.34	0.47	218	0.21	179
QUI	-0.200	-78.500	2837	295	11	0.53	0.50	1.72	0.24	138		
RAB	-4.191	152.170	184	1620	16	0.80	0.44	-0.47	0.72	260	0.93	155
RAC	50.083	18.194	209	171	9	0.49	0.47	0.97	0.21	101		
RAL	-4.220	152.202	91	83	4	0.50		0.09				
RAM	37.766	41.292	1185	197	7	0.42		0.42				
RAO	-29.252	-177.918	110	48	3	0.35		0.88				
RAR	-21.212	-159.773	28	400	14	0.88	0.79	1.15	0.68	27		
RBA	34.009	-6.841	39	254	16	0.92	0.62	0.60	0.41	11	0.82	138
RBZ	33.929	-6.840	116	237	11	0.50	0.50	0.28	0.13	167		
RCC	19.994	-75.696	100	43	3	0.52		-0.06				
RCD	44.075	-103.208	995	269	10	0.79	0.67	-0.05	0.61	236		
RCI	38.106	15.643	29	72	5	1.29		1.24				
RDJ	-22.895	-43.223	29	50	3	0.35		0.09				
RES	74.687	-94.900	15	3090	18	0.59	0.27	-0.28	0.71	39	0.31	89
REY	64.139	-21.906	44	274	10	0.58	0.35	1.91	0.69	114		
RHO	36.437	28.224	45	104	7	0.45		1.17				
RIV	-33.829	151.158	25	1006	14	0.61	0.29	0.85	0.68	338	0.25	167
RJF	45.304	1.516	410	395	13	0.29	0.28	0.20	0.12	99		
RKT	-23.118	-134.972	100	149	6	0.36		0.73				
RLO	36.167	-95.026	384	185	8	0.49		-0.37				
RMB	36.886	-90.278	147	68	4	0.67		-1.04				
RMP	41.811	12.702	380	1029	17	0.54	0.45	0.36	0.45	155	0.23	5
RMU	37.076	-110.970	1536	80	4	1.03		1.10				
ROB	44.295	7.870	806	188	9	0.63		-0.84				
ROC	43.125	-77.592	155	241	10	0.69	0.53	-0.04	0.65	56		
ROL	37.918	-91.869	200	561	13	0.49	0.42	-0.73	0.42	94		
ROM	41.903	12.513	45	412	11	0.65	0.46	1.16	0.62	242		
ROX	-45.476	169.320	106	125	3	0.19		0.79				
RSB	50.888	5.832	0	46	5	0.60		0.76				
RSL	45.688	6.626	1583	1123	15	0.63	0.39	-0.22	0.87	331	0.08	52
RUV	-15.189	-147.384	3	500	16	0.70	0.59	0.85	0.26	281	0.55	98
RXF	48.865	-115.124	4040	122	8	0.56	0.38	-0.19	0.69	42		
SAL	45.607	10.526	70	303	10	0.53	0.39	0.15	0.53	111		
SAM	39.673	66.990	704	1595	16	0.29	0.21	0.49	0.06	279	0.25	1
SAN	-33.453	-70.662	533	264	14	0.43	0.35	-0.11	0.28	55	0.31	90
SAO	36.765	-121.445	350	545	14	0.41	0.36	0.73	0.27	4	0.18	64
SAP	43.058	141.332	18	206	11	0.71	0.48	0.50	0.84	200		
SAV	-41.721	147.189	180	1470	16	0.59	0.34	1.07	0.60	339	0.25	101
SBA	-77.850	166.756	38	2148	17	0.59	0.46	1.01	0.44	52	0.29	13
SBB	34.688	-117.825	832	99	7	0.34		0.03				
SBR	-35.259	149.533	0	33	2	0.12		1.41				
SBS	36.867	10.350	127	32	2	0.68		1.47				
SCB	43.717	-79.233	153	178	7	0.61		0.49				
SCG	16.029	-61.681	646	110	9	0.71	0.59	0.44	0.66	65		
SCH	54.817	-66.783	540	2269	18	0.39	0.36	-0.40	0.21	115	0.07	37
SCM	61.833	-147.328	1020	667	14	0.39	0.35	0.20	0.13	180	0.31	161
SCO	70.483	-21.950	69	84	2	0.04		1.14				
SCP	40.795	-77.865	352	347	9	0.94	0.53	-0.23	1.15	80		
SDA	42.016	19.499	0	67	5	0.44		0.14				

TABLE 2. (continued)

CODE	LAT	LONG	ELEV	P-WAVE STATION CORRECTION								
				NOBS	NW	RMS0	RMS1	A0	A1	E1	A2	E2
SDB	-14.926	13.572	1781	802	18	0.63	0.45	0.22	0.53	62	0.21	91
SDV	8.886	-70.633	1580	127	9	0.58	0.35	-0.22	0.71	35		
SEA	47.655	-122.308	30	147	8	0.70		2.25				
SEH	23.167	77.083	0	61	5	0.26		1.04				
SEM	50.408	80.250	209	2308	18	0.64	0.30	-0.21	0.75	241	0.15	88
SEO	37.567	126.967	86	228	11	0.63	0.56	0.28	0.40	102		
SES	50.396	-111.042	770	2583	16	0.33	0.26	-0.56	0.27	70	0.17	150
SET	36.200	5.400	1000	201	11	0.44	0.43	-0.07	0.12	35		
SEY	62.900	152.400	210	593	13	0.33	0.27	0.09	0.33	258		
SFA	47.123	-70.827	232	1014	17	0.61	0.48	-0.03	0.34	152	0.35	24
SFF	-41.337	146.307	213	187	8	0.34		1.27				
SFR	37.787	-122.389	8	53	4	0.32		1.30				
SFS	36.462	-6.205	24	99	8	1.09		1.51				
SGR	47.709	-0.923	90	105	9	0.70	0.51	0.17	0.76	298		
SHD	36.433	54.942	1500	390	10	0.39	0.32	0.62	0.45	3		
SHE	40.633	48.633	0	262	7	0.32		1.93				
SHF	46.552	-72.763	60	141	4	0.37		-0.48				
SHI	29.644	52.526	1595	3365	18	0.32	0.31	-0.28	0.08	310	0.11	163
SHK	34.530	132.678	285	1769	14	0.51	0.49	-0.32	0.15	172		
SHL	25.567	91.883	1600	3489	18	0.52	0.30	-0.57	0.53	167	0.24	22
SIA	34.248	108.920	0	158	7	0.46		0.76				
SIC	50.189	-66.740	283	720	17	0.66	0.55	-0.08	0.29	108	0.44	12
SID	63.786	-18.058	26	181	9	0.71	0.32	1.60	1.10	7		
SIM	44.950	34.117	277	1769	17	0.44	0.38	0.64	0.08	270	0.30	155
SIT	57.057	-135.324	19	829	16	0.53	0.32	0.91	0.57	1	0.17	133
SJG	18.112	-66.150	457	714	15	0.83	0.67	-0.63	0.78	45	0.11	62
SJP	18.382	-66.118	80	88	3	1.30		-0.48				
SKA	63.580	12.280	580	656	14	0.78	0.49	-0.07	0.80	303	0.48	109
SKI	17.333	-62.739	306	133	10	0.63	0.58	0.31	0.37	43		
SKO	41.972	21.440	346	1765	17	0.34	0.30	0.01	0.12	250	0.22	17
SKR	50.667	156.100	250	660	13	0.85	0.42	-0.34	1.10	213		
SLA	-24.728	-65.494	0	43	3	0.44		-0.77				
SLC	40.765	-111.848	1425	731	16	0.41	0.25	0.09	0.20	87	0.39	159
SLD	37.075	-121.221	443	814	14	0.35	0.30	1.22	0.27	2		
SLL	60.477	13.323	420	215	9	0.53		-0.28				
SLM	38.636	-90.236	161	293	6	0.31		-0.18				
SMF	46.645	3.841	459	363	12	0.40	0.38	-0.17	0.15	242		
SMY	52.731	174.103	58	334	11	0.91	0.34	-0.19	1.31	237		
SNA	-70.315	-2.325	57	391	13	0.73	0.55	0.11	0.76	11		
SNG	7.173	100.620	4	376	12	0.80	0.44	0.27	1.00	70		
SOC	43.583	39.717	192	994	16	0.76	0.51	0.34	0.56	343	0.67	135
SOD	67.371	26.629	181	4982	18	0.24	0.20	-0.24	0.18	128	0.04	163
SOF	42.685	23.334	546	720	16	0.56	0.29	0.54	0.17	144	0.63	64
SOP	47.683	16.558	260	1192	15	0.49	0.30	-0.35	0.35	20	0.31	15
SOR	22.792	-83.008	206	95	5	0.21		0.40				
SPA	-90.000	0.	2927	1857	16	0.73	0.59	-0.48	0.57	281	0.18	24
SPC	49.188	20.245	1772	395	14	0.50	0.34	1.37	0.29	344	0.56	87
SPF	43.564	6.696	340	920	15	0.42	0.34	0.31	0.30	274	0.09	160
SPK	-43.038	146.275	425	58	6	0.89		1.71				
SPO	47.732	-117.344	713	287	6	0.27		0.73				
SRI	36.758	49.383	243	890	13	0.37	0.25	0.80	0.35	319	0.32	64
SRO	47.813	18.313	150	792	15	0.57	0.44	1.18	0.33	50	0.32	14
SRY	35.608	139.274	254	1328	14	0.69	0.43	-0.09	0.65	56	0.72	100
SSA	44.531	21.559	0	70	7	0.78		-1.68				
SSB	45.279	4.542	700	173	9	0.49	0.28	0.38	0.64	300		
SSC	48.584	-0.107	300	2382	16	0.39	0.27	0.10	0.36	264	0.04	157
SSF	47.061	3.507	360	3005	17	0.36	0.26	0.02	0.22	267	0.27	177
SSR	44.531	21.531	0	196	8	0.99	0.15	0.06	2.59	209		
SSS	13.681	-89.198	665	49	3	0.37		1.85				
STC	36.633	-121.233	259	140	6	0.38		1.70				
STG	-42.848	146.207	350	75	6	0.69		1.20				
STH	18.078	-76.814	427	36	3	0.53		0.63				
STJ	47.572	-52.733	62	733	16	0.57	0.47	0.15	0.26	317	0.47	26
STK	-31.882	141.592	213	1289	17	0.42	0.32	-0.23	0.21	93	0.30	92
STR	48.585	7.766	135	1541	15	0.50	0.24	0.65	0.59	1	0.35	143
STS	42.886	-8.551	265	30	2	0.22		0.41				
STU	48.772	9.195	360	1286	16	0.61	0.35	-0.26	0.62	5	0.35	159
STV	44.244	7.324	985	68	5	0.68		-1.62				
SUD	46.467	-80.967	267	391	14	0.64	0.39	0.17	0.32	26	0.65	73
SUR	-32.380	20.812	1765	223	13	0.47	0.47	0.78	0.07	117		
SUV	-18.149	178.457	6	35	3	0.66		0.83				
SVA	-18.117	178.458	48	46	3	0.06		1.05				
SVE	56.810	60.637	275	3588	18	0.37	0.29	0.15	0.28	180	0.20	81
SVM	32.779	-108.297	1932	55	4	0.34		1.06				
SVT	13.168	-61.245	38	88	5	0.67		0.37				
SVW	61.108	-155.622	762	1109	15	0.84	0.20	0.13	1.04	299	0.15	170
SWV	-31.883	116.065	80	257	9	0.64		-0.11				
SYO	-69.006	39.503	23	438	13	0.83	0.56	-0.16	1.02	321		
TAB	38.067	46.327	1430	2184	18	0.49	0.37	0.74	0.42	68	0.08	30
TAC	19.405	-99.194	2297	292	10	0.72	0.65	1.05	0.44	141		
TAF	34.814	-2.414	820	386	16	0.66	0.45	0.59	0.53	120	0.38	104
TAM	22.792	5.523	1395	988	18	0.46	0.44	-0.13	0.16	158	0.14	129
TAN	-18.917	47.552	1375	518	11	0.78	0.20	1.12	1.13	235		
TAS	41.325	69.295	470	3277	18	0.35	0.28	0.50	0.22	201	0.23	71
TAU	-42.910	147.320	132	1841	16	0.66	0.42	0.95	0.55	25	0.45	96

TABLE 2. (continued)

CODE	LAT	LONG	ELEV	P-WAVE STATION CORRECTION								
				NOBS	NW	RMS0	RMS1	A0	A1	E1	A2	E2
TAV	-4.231	152.220	31	120	7	0.34		0.11				
TBZ	40.994	39.776	57	42	3	0.72		0.68				
TCF	46.288	2.214	640	1593	16	0.29	0.25	0.24	0.21	175	0.18	6
TDJ	11.787	42.890	50	39	4	0.58		1.92				
TEC	34.850	-1.283	0	38	2	0.21		0.89				
TEH	35.738	51.386	1360	1487	18	0.51	0.43	0.77	0.32	30	0.22	1
TEN	28.464	-16.245	1	137	10	0.46	0.31	2.31	0.40	250		
TET	-16.146	33.577	153	598	14	0.77	0.44	0.78	0.62	138	0.83	144
TFO	34.268	-111.270	1492	1544	16	0.35	0.24	0.55	0.30	42	0.28	112
TGI	32.963	59.193	1800	428	11	0.40	0.38	0.45	0.20	327		
THO	33.875	-111.874	1134	81	4	0.28		1.12				
THT	-17.569	-149.574	337	101	6	0.33		1.63				
TIF	41.717	44.800	399	1516	18	0.47	0.45	0.88	0.09	18	0.19	144
TIK	71.633	128.867	25	3829	17	0.57	0.31	-0.86	0.45	298	0.43	130
TIM	45.737	21.222	88	114	9	0.37	0.36	1.52	0.14	86		
TIO	30.927	-7.262	1335	559	17	0.49	0.45	0.78	0.27	188	0.09	170
TIR	41.347	19.867	197	602	16	0.66	0.52	0.66	0.57	227	0.17	5
TJC	37.217	-104.691	2103	256	7	0.40		1.20				
TLG	43.267	77.383	850	619	13	0.74	0.56	0.27	0.67	84		
TLL	-30.167	-70.804	2200	231	14	0.36	0.26	-0.21	0.28	6	0.40	111
TLS	-5.310	150.045	40	186	10	0.44	0.42	0.79	0.19	286		
TMT	41.811	-72.799	290	210	11	0.59	0.41	0.85	0.69	94		
TNG	-6.183	106.500	14	277	11	1.17	1.11	0.34	0.88	223		
TNN	65.257	-151.912	504	355	11	0.59	0.54	0.76	0.35	333		
TNO	45.059	7.697	260	30	2	0.20		-0.63				
TNP	38.082	-117.218	1932	932	15	0.40	0.28	0.30	0.27	70	0.35	128
TNS	50.224	8.449	815	269	9	0.62		0.76				
TOA	62.105	-146.172	909	692	12	0.31	0.24	0.47	0.32	39		
TOL	39.881	-4.049	480	1362	16	0.42	0.32	0.77	0.25	337	0.28	135
TOO	-37.571	145.491	604	3183	18	0.55	0.44	0.24	0.39	280	0.27	101
TOV	9.793	-69.793	650	139	9	0.82	0.34	0.51	1.32	43		
TPH	38.075	-117.222	1890	172	6	0.39		0.39				
TPM	18.983	-99.062	1500	177	8	0.72		1.54				
TPT	-14.984	-147.619	3	854	17	0.63	0.53	0.90	0.35	325	0.47	91
TRD	8.483	76.950	0	172	8	0.87		1.02				
TRI	45.709	13.764	126	1336	16	0.35	0.27	-0.23	0.26	268	0.12	140
TRJ	-21.513	-64.776	2100	52	5	1.09		-0.35				
TRM	44.260	-70.255	113	65	6	0.60		0.85				
TRN	10.649	-61.403	24	619	14	1.38	0.36	0.25	1.79	107	0.53	31
TRO	69.632	18.928	15	3093	18	0.30	0.17	0.29	0.33	267	0.08	112
TRR	-42.304	146.450	579	980	15	0.65	0.49	1.30	0.25	331	0.53	92
TRT	-7.650	112.500	0	127	7	0.66		0.36				
TSI	3.509	98.562	0	54	5	0.41		0.35				
TSK	36.211	140.110	280	1955	14	0.80	0.37	-0.18	1.01	89	0.38	126
TTA	62.930	-156.022	914	679	14	0.68	0.35	-0.34	0.79	311		
TTN	22.750	121.150	9	149	8	1.21		4.06				
TUA	-38.808	177.151	274	37	2	0.12		-0.18				
TUC	32.310	-110.782	985	2885	17	0.27	0.24	0.14	0.18	41	0.06	126
TUL	35.911	-95.792	256	2089	16	0.35	0.32	-0.52	0.12	194	0.17	76
TUM	47.015	-122.908	20	345	14	0.71	0.64	0.46	0.44	321		
TUP	54.433	119.900	0	1615	16	0.53	0.24	0.05	0.54	245	0.35	113
TVO	-17.782	-149.252	660	525	16	0.77	0.64	1.64	0.55	211	0.34	122
TYS	38.515	-90.568	175	71	5	0.39		-0.29				
TZZ	-5.268	141.221	700	48	4	0.39		-0.86				
UAV	8.604	-71.145	1550	278	13	0.70	0.55	0.04	0.62	28		
UBO	40.322	-109.569	1596	1908	16	0.46	0.25	-0.19	0.34	358	0.38	136
UCC	50.798	4.359	105	963	16	0.59	0.46	1.18	0.40	23	0.43	94
UCT	41.832	-72.251	149	285	11	0.61	0.48	0.83	0.60	92		
UDD	60.090	13.607	240	345	13	0.58	0.47	-0.58	0.46	286		
UDI	46.065	13.237	112	66	4	0.45		-0.48				
UKI	39.137	-123.211	199	190	9	0.47		1.61				
UME	63.815	20.237	16	4194	17	0.38	0.26	-0.39	0.28	232	0.27	89
UNM	19.329	-99.178	2257	154	7	0.76		0.92				
UPP	59.858	17.627	14	4180	17	0.27	0.23	-0.48	0.17	260	0.02	148
URS	33.538	133.489	25	47	4	0.35		0.78				
UZH	48.633	22.300	159	3018	17	0.31	0.25	0.59	0.13	222	0.20	99
VAH	-15.237	-147.636	3	681	16	0.59	0.46	0.79	0.24	261	0.54	97
VAL	51.939	-10.244	14	947	15	0.80	0.75	0.94	0.18	315	0.33	114
VAM	35.407	24.200	225	644	14	0.92	0.54	0.72	0.91	202	0.46	92
VAN	37.950	58.100	250	1643	17	0.53	0.30	-0.19	0.58	45	0.43	123
VAR	25.300	83.017	88	647	12	0.65	0.42	-0.52	0.69	146		
VAY	41.321	22.570	168	996	17	0.44	0.37	-0.07	0.25	214	0.31	27
VCA	-28.741	-68.202	0	35	2	0.38		0.13				
VHM	17.177	-96.745	1829	293	11	0.50	0.45	1.45	0.28	199		
VHO	17.236	-96.732	1685	91	5	0.50		1.08				

TABLE 2. (continued)

CODE	LAT	LONG	ELEV	P-WAVE STATION CORRECTION								
				NOBS	NW	RMS0	RMS1	A0	A1	E1	A2	E2
VIC	48.519	-123.415	197	1187	16	0.49	0.30	0.13	0.41	267	0.38	176
VIE	48.248	16.362	198	1160	15	0.54	0.26	0.20	0.58	54	0.21	37
VIS	17.717	83.300	41	297	9	0.47		0.72				
VKA	48.265	16.318	400	1852	17	0.49	0.31	0.10	0.42	56	0.25	32
VLA	43.120	131.893	75	1853	14	0.59	0.34	0.21	0.74	175	0.13	133
VLN	-13.887	167.542	18	45	4	0.73		0.56				
VLO	40.469	19.495	0	34	3	0.35		0.05				
VLS	38.177	20.590	375	766	14	0.63	0.42	0.05	0.83	217	0.49	7
VLV	-39.790	-73.276	12	74	6	1.18		0.16				
VOU	46.399	5.651	495	583	12	0.37	0.25	0.26	0.44	313		
VRI	45.870	26.725	400	1786	17	0.56	0.46	0.55	0.43	56	0.16	105
VTS	42.600	23.200	0	46	3	0.40		0.72				
VTY	-19.076	47.539	1423	228	9	1.00	0.34	1.54	1.45	244		
VUL	-4.283	152.146	332	102	6	0.52		0.28				
VUN	-18.043	178.464	160	260	6	0.58		0.95				
VYB	60.717	28.800	0	198	8	0.38		-0.88				
WAB	-5.495	143.728	2032	871	14	0.84	0.46	1.12	1.21	220		
WAM	-36.193	148.883	200	69	5	0.37		0.46				
WAN	-4.194	152.176	25	67	5	0.44		0.20				
WAR	52.242	21.024	110	102	7	0.48		0.89				
WAS	38.892	-77.033	0	59	3	0.61		-0.04				
WB2	-19.944	134.353	366	143	7	0.50		-1.34				
WB3	-19.925	134.357	366	200	8	0.31		-1.15				
WB4	-19.905	134.361	366	43	3	0.45		-1.31				
WBN	-26.140	126.578	457	30	2	0.79		0.09				
WCB	-19.935	134.357	366	878	13	0.49	0.44	-1.25	0.33	256		
WCK	36.934	-88.874	137	40	3	0.36		-0.15				
WCN	39.311	-119.756	1709	390	12	0.36	0.21	0.83	0.44	38		
WDC	40.580	-122.540	300	1412	16	0.93	0.24	-0.35	1.16	289	0.31	173
WDY	35.700	-118.843	490	68	2	0.04		-0.18				
WEL	-41.286	174.768	122	667	11	0.69	0.57	0.16	0.52	98		
WES	42.385	-71.322	60	700	15	0.51	0.42	0.77	0.39	126	0.15	59
WET	49.145	12.880	613	381	12	0.50	0.27	-0.06	0.75	10		
WGL	17.985	79.530	280	135	7	0.37		0.10				
WIL	-66.259	110.527	10	203	11	0.45	0.44	0.27	0.09	198		
WIN	-22.567	17.100	1728	970	17	0.46	0.40	0.62	0.30	50	0.12	40
WIT	52.813	6.668	17	1745	15	0.43	0.32	1.40	0.29	344	0.28	158
WKR	35.814	-120.511	503	152	8	0.12		1.35				
WKU	34.188	135.173	10	127	8	0.41		0.50				
WLF	49.665	6.152	0	61	4	0.30		2.02				
WLO	34.065	-97.370	284	42	3	0.22		0.50				
WLS	48.413	7.354	775	1845	18	0.43	0.23	0.04	0.48	340	0.19	164
WMO	34.718	-98.589	505	1094	13	0.48	0.28	-0.76	0.51	345		
WOL	51.317	-1.217	0	545	14	0.48	0.43	0.84	0.34	188		
WPM	46.752	-89.555	193	48	3	0.41		0.26				
WRA	-19.944	134.364	360	2563	16	0.36	0.25	-1.13	0.34	253	0.17	126
WRM	49.833	5.381	242	405	13	0.88	0.88	2.35	0.21	11		
WRS	34.150	71.408	343	2316	18	0.55	0.33	-0.14	0.44	242	0.44	84
WSC	39.050	-77.124	120	409	13	0.62	0.42	-0.13	0.57	126	0.22	27
WTS	51.996	6.810	43	444	16	0.45	0.39	0.82	0.27	156	0.28	145
WTZ	-37.985	176.988	43	182	6	1.01		-0.03				
WUC	30.543	114.350	26	68	4	0.42		0.80				
WYO	42.778	-109.556	2190	45	2	0.64		-0.92				
YAK	62.017	129.717	125	3369	16	0.53	0.45	-0.86	0.32	256	0.29	20
YER	37.135	28.283	730	401	8	0.36		0.07				
YKA	62.493	-114.605	200	659	15	0.48	0.33	0.88	0.46	358	0.24	72
YKC	62.478	-114.478	198	2816	16	0.47	0.30	-0.65	0.46	330	0.04	58
YKM	48.862	-115.712	4950	66	6	0.75	0.17	-0.24	1.54	16		
YKT	59.369	-138.877	336	54	4	0.38		0.06				
YOU	-34.278	148.382	503	747	13	0.34	0.30	0.47	0.22	137		
YSS	47.017	142.717	75	2798	15	0.36	0.27	0.51	0.14	324	0.25	140
ZAG	45.817	15.983	155	667	15	0.56	0.48	1.00	0.35	93	0.26	146
ZAK	50.383	103.283	0	3173	18	0.44	0.29	0.44	0.39	287	0.18	112
ZLP	-16.270	-68.118	4398	161	11	0.66	0.58	-0.73	0.47	115		
ZOBO	-16.270	-68.125	4450	49	4	0.66		-1.14				
ZSC	31.097	121.187	100	147	7	0.46		0.36				
ZST	48.196	17.103	250	415	15	0.55	0.35	0.53	0.61	22	0.17	155
ZUL	47.481	8.390	740	929	15	0.54	0.39	-1.09	0.64	346	0.02	135
ZUR	47.369	8.580	604	104	6	0.45		-0.41				

See text for explanation of headings and contents of the table.

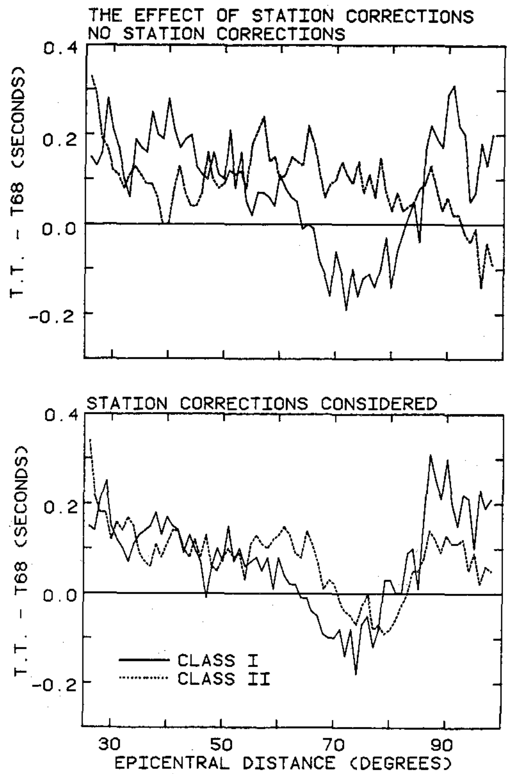

Fig. 4. The effect of introduction of station corrections on the travel time curves presented, as in Figure 2, in terms of deviations from 1968 tables. Station corrections not only reduce the roughness, but also are capable of changing the trend over a large range of distances, decreasing the diffrence between the travel times for class I and class II events.

Because of the better geographical coverage, and with the appropriate reservations, we recommend the travel times for the class I events, corrected for station effects, as the best estimate of teleseismic travel times for surface focus P waves.

Figures 5a-5h show examples of the azimuthal dependence of station residuals. The principal point is to demonstrate the variety and range of the station terms as well as the consistency of the residuals for the class I and class II events. Although these figures show stations reporting a relatively large number of observations with good azimuthal coverage, the selection in terms of similarity between the two types of residuals is typical. From this we conclude that the source effect is either not as important as might have been thought, or as already mentioned, it has been, in part, absorbed by the process of relocation of events. In either case, the station residuals listed in Table 2 would seem to be dominated by the upper mantle and, perhaps, crustal structure in the vicinity of the station.

Figure 5a represents a station with nearly no azimuthal dependence of residuals and also a very small constant term. Figure 5b, on the other hand, shows a peak-to-peak variation of nearly 4 s. The residuals for class I and II events differ in the window centered on an azimuth of 330° by more than 2 s, but in the other five windows for which observations of both types exist, the data are very close to each other. Figure 5b represents a rare example of a station dominated by class II events.

Figure 5c is an example of a station dominated by the A_0 and A_1 terms, with the coefficient A_2 being virtually zero, while in Figure 5d the latter term dominates. Figures 5e and 5f are examples of stations with relatively large second azimuthal terms. Figures 5g and 5h are shown to demonstrate the consistency of the residual pattern over fairly large distances: the two stations in the Canadian Arctic are nearly 900 km apart, and yet the magnitude and the phase of the anomalies are very similar.

The consistency of different terms in our table of station corrections can be more easily judged from a map display. Figure 6a shows the size and distribution of the azimuth-independent term over the large part of the North American continent. The stations displayed reported at least 700 observations distributed in at least 10 azimuth windows. Squares designate late, or slow, stations; triangles represent early, or fast, stations. The size of the symbol is proportional to that of the anomaly; the scale for +1 and -1 s is shown.

The arrivals are systematically late for stations in the Appalachians. Most of the stations in the Great Plains and in Canada east of the Rocky Mountains are fast. Nevada and California are very slow. This picture is in excellent agreement with the results of Herrin and Taggart [1968, Figure 2].

Figure 6b displays the variation in the first azimuthal term. The arrow points toward the slow direction, and its length is proportional to the A_1 coefficient (see inset for an arrow corrresponding to 1 s anomaly). To be included in this figure a station had to report at least 1000 observations for at least 15 azimuth windows. While the stations in the east and north (including Alaska) show consistency over large distances, the situation in the west is more complex. If we discard the coastal stations, which show great variability in their pattern, we notice that there are two populations of arrows that represent a very consistent pattern. One group of relatively large anomalies (~0.5 s) points nearly due north, and the other, consisting of anomalies of about 0.25 s, points in the direction N45°E. The two types of arrows are intermixed, but the populations are well defined. Clearly, an attempt should be made to correlate this observation with other kinds of geophysical and geological data.

Figure 6c shows the second azimuthal term. The criteria for displaying a station are the same as in the case of Figure 6b and remain so for all the figures to follow. The small square designates the position of the station and the line represents the slow azimuth. There is a great deal of regional consistency in the second azimuthal term. In the western United States and Canada the slow direction remains similar over an area about 2000 km long in the NS direction and 1000 km wide from east to west. There is some indication of a gradual rotation toward north-south slow directions as one progresses from Mexico to Canada. A group of stations near the coast of southern California represents an

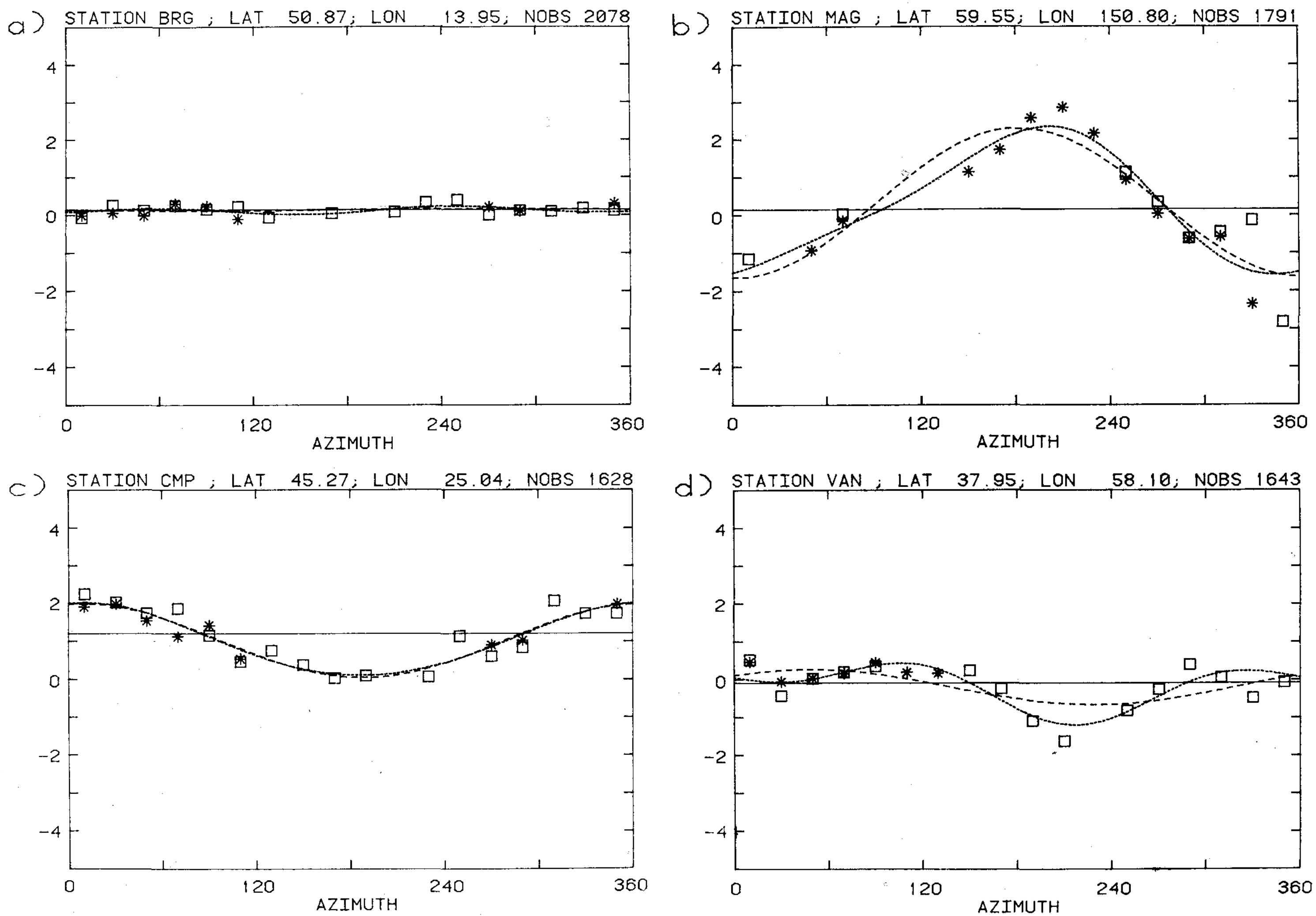
a) STATION BRG ; LAT 50.87; LON 13.95; NOBS 2078
b) STATION MAG ; LAT 59.55; LON 150.80; NOBS 1791
c) STATION CMP ; LAT 45.27; LON 25.04; NOBS 1628
d) STATION VAN ; LAT 37.95; LON 58.10; NOBS 1643
4
2
0
-2
-4
0
120
240
360
AZIMUTH

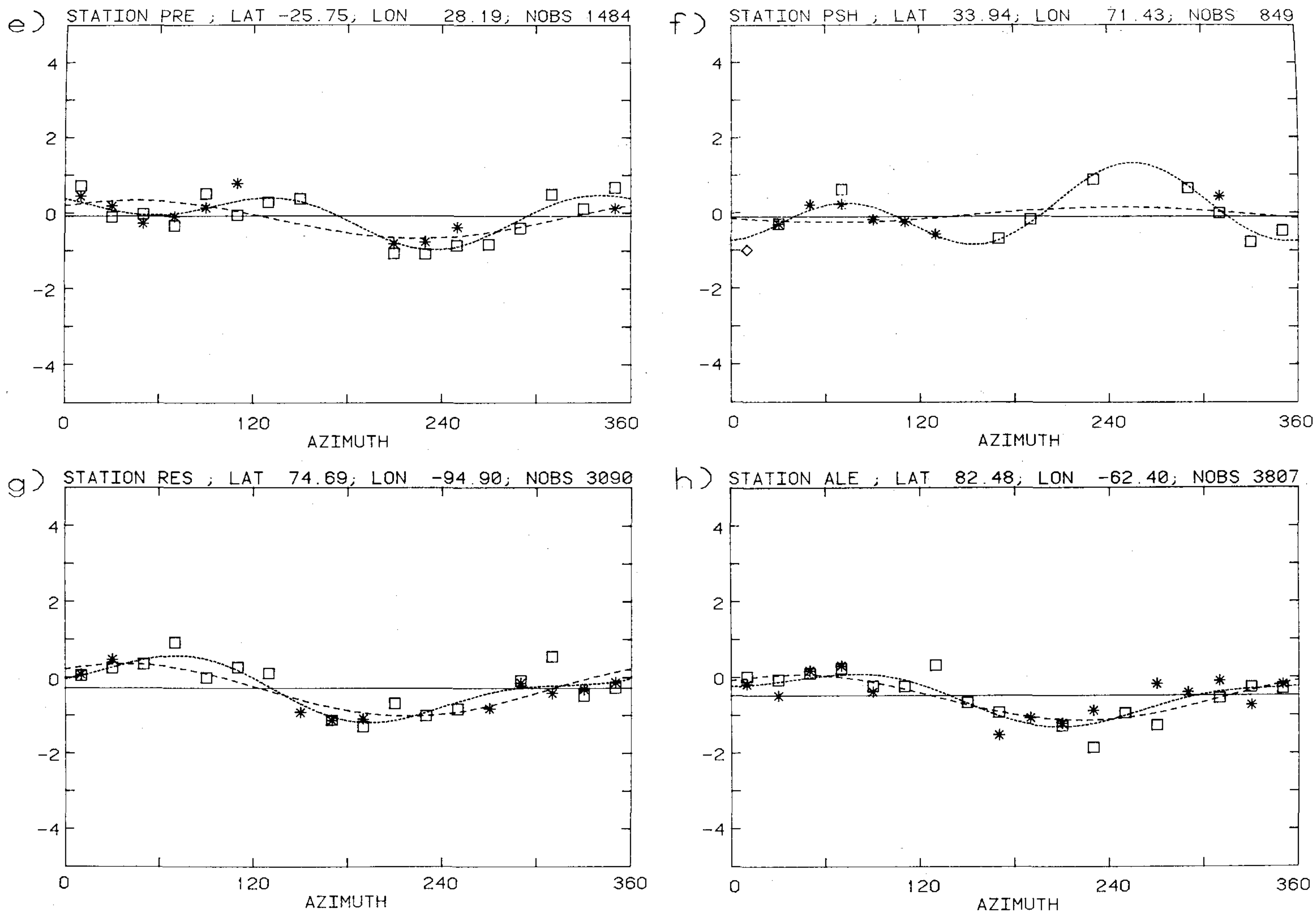

Fig. 5. Examples of station residuals as a function of azimuth illustrating variability in the ralative importance of different station correction terms. For details see caption to Figure 3.

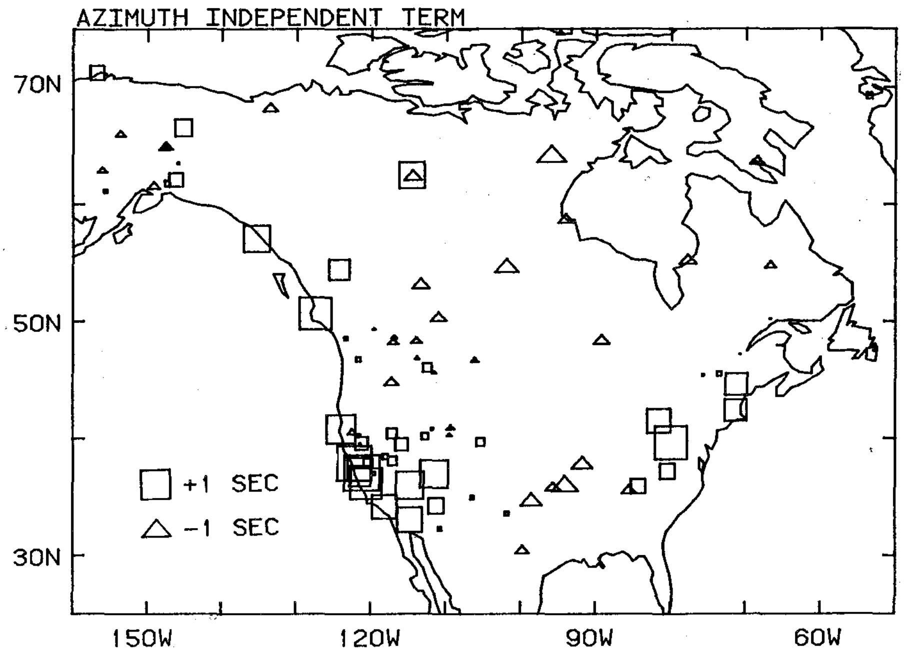

Fig. 6a. Distribution of the constant station correction term for stations in the North American continent. Only stations with at least 700 observations distributed among at least 14 azimuthal windows are displayed. The size of a symbol is proportional to the anomaly.

exception: the change in direction by about 60° is very abrupt. One of the sources of a perceptible second azimuthal term could be anisotropy. The fast direction in southern California is parallel to the direction of motion of the Pacific plate. This has also been found in studies of P_n in southern California and has been attributed to upper mantle anisotropy [Vetter and Minster, 1981]. In studies of the anisotropy of olivine the fast axis is parallel to the flow direction [Christensen and Salisbury, 1980]. This raises the possibility that the second azimuthal

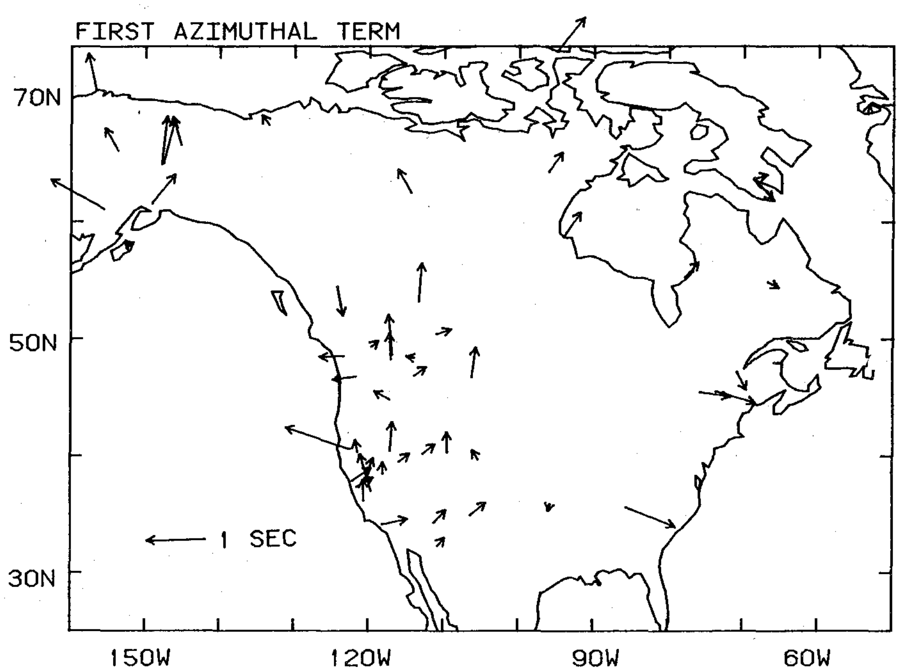

Fig. 6b. Distribution of the first azimuthal term in station anomalies for stations in the North American continent. Arrows point toward the slow direction, and their length is proportional to the anomaly. Only stations with at least 1000 observations distributed among at least 15 azimuth windows are displayed.

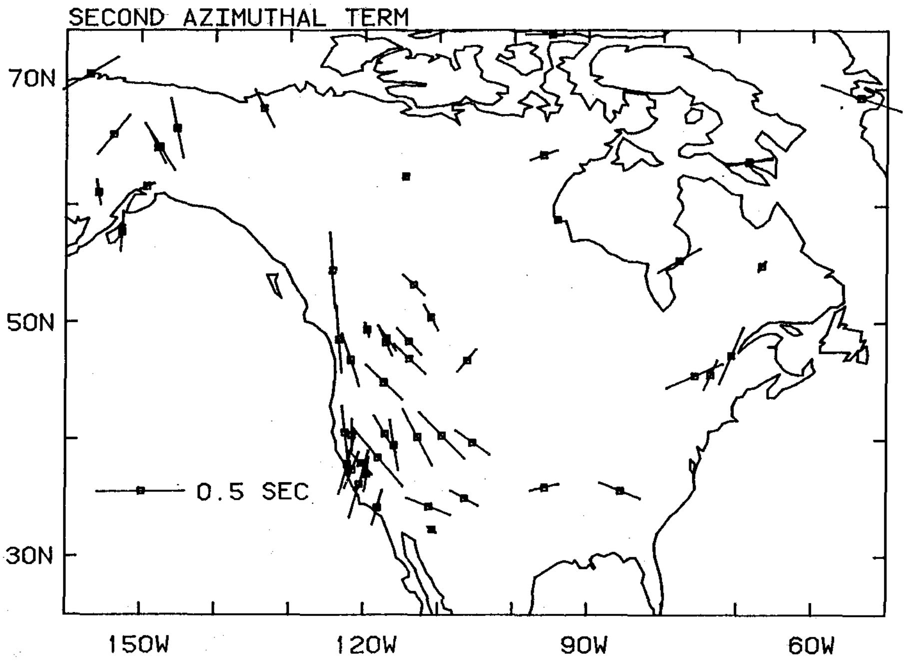

Fig. 6c. Distribution of the second azimuthal term in station anomalies for stations in the North American continent. The line centered over a station is aligned in the slow direction and its length is proportional to the anomaly. Observational requirements are the same as in Figure 6b.

term can be used to map the direction of flow in the mantle.

Figure 7a shows the azimuth-independent term for Europe. Stations distributed along the Alpide belt are generally slow; station AKU on Iceland has a positive residual of over 2 s. Stations on the Baltic Shield are generally fast. Thus the familiar pattern, first detected by Cleary and Hales [1966], is well reproduced. The most striking feature of Figure 7b is the fanlike pattern of the arrows pointing away from the Alpide belt for stations between longitudes 0 and 30°E. For the Scandinavian stations the slow direction is toward the west, although the magnitude of the arrows there is rather small. Association of the fast-slow direction with the

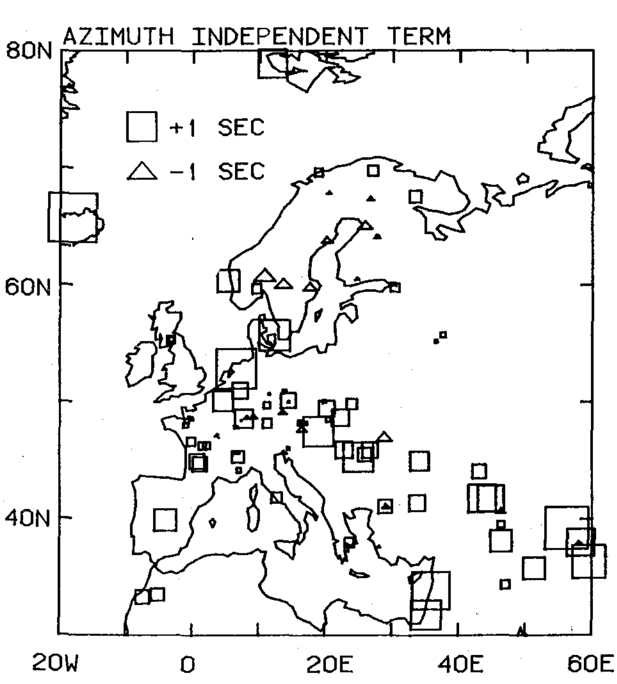

Fig. 7a. Same as Figure 6a but for Europe. Observational threshold: 1000 observations in 15 azimuthal windows.

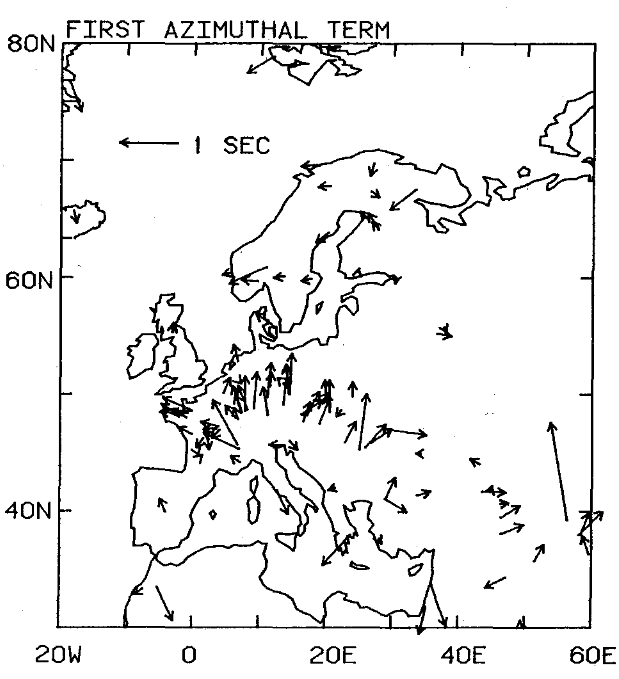

Fig. 7b. Same as Figure 6b but for Europe.

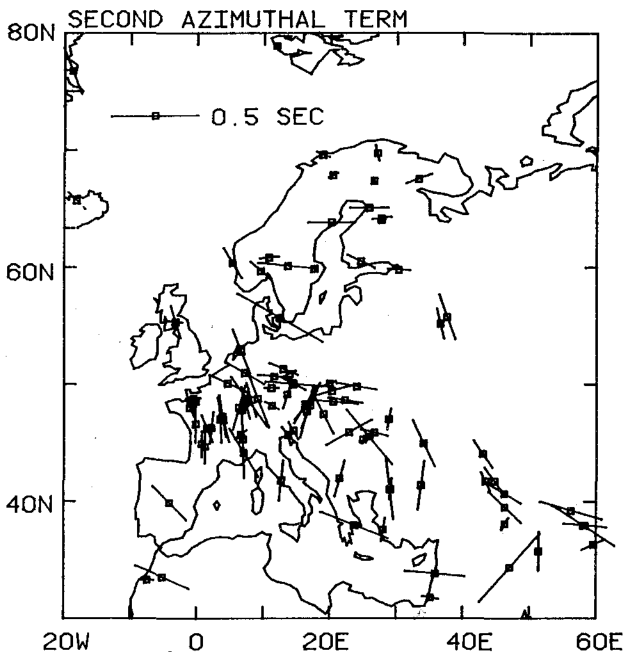

Fig. 7c. Same as Figure 6c but for Europe.

major tectonic feature of Europe can also be seen in Figure 7c, which displays the second azimuthal term. The slow direction here is mostly parallel to the Alpide belt, with the trend continuing to the east, although the picture in western Europe is less clear than in Figure 7b. Thus the fast direction is perpendicular to the Alpide arc, and this reinforces the negative anomaly produced by the first azimuthal term. If the proposed association of the azimuthal variations of the travel time anomalies with the Alpide belt is correct, the structure associated with the Alps would have to extend well into the upper mantle.

On a global scale, the azimuth independent term (Figure 8a) correlates with the tectonic nature of a given region, as pointed out by Cleary and Hales [1966]: the shields are fast (western and central Australia, Siberia, South Africa, Canada), and tectonically active regions are slow (Tasmania, the west coast of North America, the Middle East, Iceland).
There seems to be a tendency among the coastal stations for the slow direction to point toward the sea: this might be associated with the relative slowness of the downdip propagation of the waves that encounter the thickening crust and possible depression of upper mantle iso-velocity surfaces. In any case, the first azimuthal term has to do with major structures in the crust and upper mantle. A simpler picture emerges from the distribution of the second azimuthal term. There are clusters of stations that show very similar behavior: Tasmania and southern and western Australia, southern Africa, a continuation of the Alpide belt into Asia, most of the Siberian stations and India, for example.

The density of station distribution is, on the global scale, much lower than that for Europe or the western United States, and therefore we do not have an opportunity to observe in comparable detail some of the gradual and sometimes abrupt but consistent changes in the pattern of different terms in station anomalies.

Establishment of the fact that under favorable circumstances, the azimuth-dependent terms show a high degree of consistency and relate to tectonic features brings the promise of an additional tool in studying the heterogeneity and anisotropy of the mantle.

The slow directions found from the second

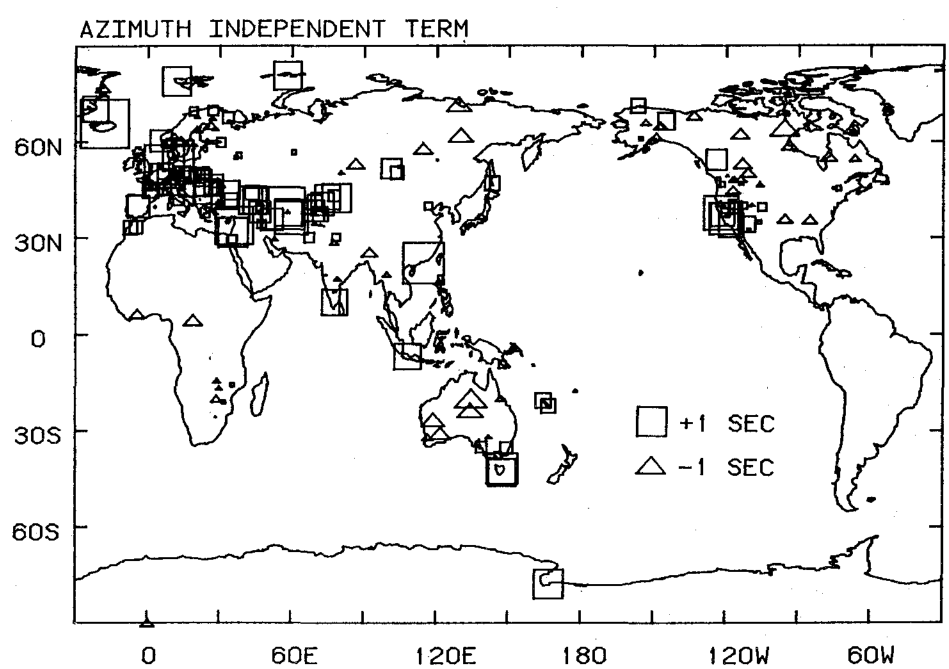

Fig. 8a. Global distribution of the constant correction term. For details see caption to Figure 6a. Observational threshold 1000 observations in 15 azimuthal windows.

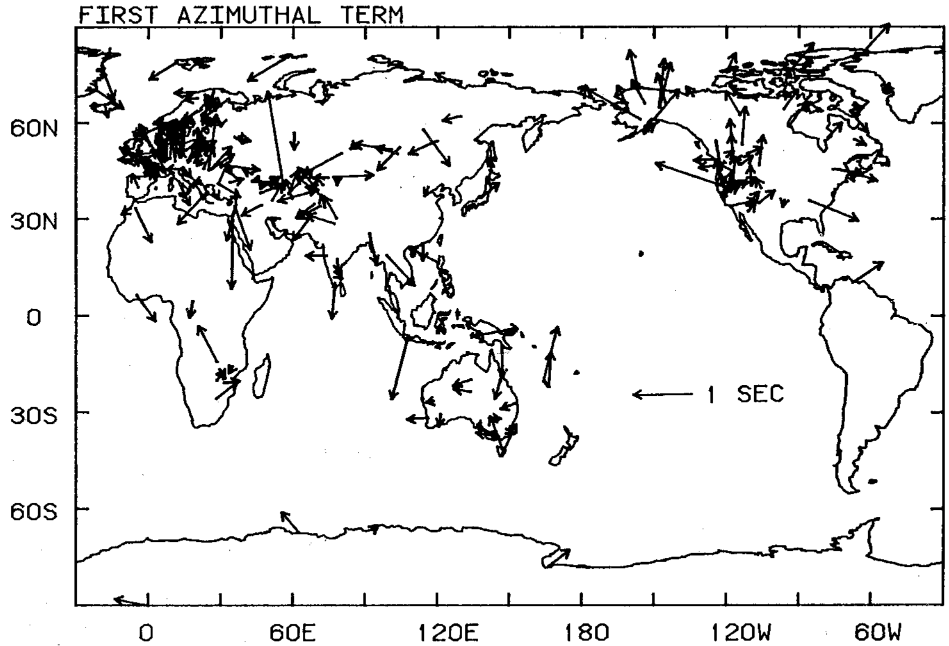

Fig. 8b. Global distribution of the first azimuthal term. For details see caption to Figure 6b.

azimuthal term bear an interesting and potentially important relationship to the direction of principal stresses in the crust. For example, the direction of greatest principal compression is NNE-SSW in southern California, EW in the southern midcontinent and NW-SE in the Colorado Plateau [Zoback and Zoback, 1980]. The axes of horizontal extension are NW-SE in the Basin and Range province and SW-NE in the Colorado Rocky Mountains. These directions are roughly parallel with the slow directions of the second azimuthal station term. The principal stress axes are close to NS in the Pacific Northwest, swinging to NW-SE in the northern Rocky Mountains and to SW-NE in the northwestern midcontinent. The station terms show the same trend. The slow directions in South Africa and southern Australia are more-or-less normal to the African Rift and the Tertiary basalt trend in Australia, respectively. Crustal stress presum-

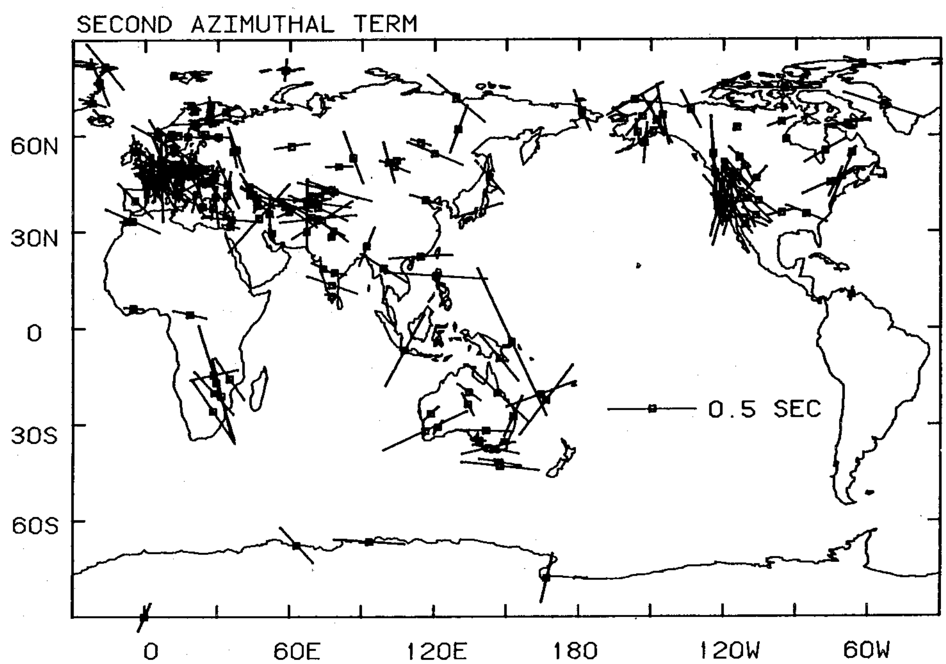

Fig. 8c. Global distribution of the second azimuthal term. For details see caption to Figure 6c.

ably is at least partially the result of mantle flow. The stress or flow-induced orientation of crystals in the upper mantle should therefore be related to stress directions in the overlying crust.

Acknowledgments. It is a great pleasure for us to dedicate this paper to Anton Hales who, in large measure, is responsible for its existence. Anton's dedication to the understanding of all of the uncertainties and subtleties in the travel time and location problems was a constant source of inspiration to us, and his personal advice and vast experience were tapped on many occasions. His studies with John Cleary provided many insights which we have profited from. Alan Douglas provided us with a detailed critique of our earlier travel time studies and convinced us that relocation of many events was a prerequisite for further progress in this field. This research was supported by National Science Foundation grants EAR81-20944 (Harvard) and EAR77-14675 (Caltech). Contribution 3801 of the Division of Geological and Planetary Sciences, California Institute of Technology, Pasadena, California 91125.

References

Carder, D. S., Travel times from Central Pacific nuclear explosions and inferred mantle structure, Bull. Seismol. Soc. Am., 54, 2271-2294, 1964.

Chinnery, M. A., Velocity anomalies in the lower mantle, Phys. Earth Planet Inter., 2, 1-10, 1969.

Christensen, N. I., and M. H. Salisbury, Seismic anisotropy in the oceanic upper mantle: Evidence from the Bay of Islands ophiolite complex, J. Geophys. Res., 84, 4601-4610, 1979.

Cleary, J., and A. L. Hales, An analysis of the travel times of P waves to North American stations, in the distance range 30° to 100°, Bull. Seismol. Soc. Am., 56, 467-489, 1966.

Davies, D., and D. P. McKenzie, Seismic travel time residuals and plates, Geophys. J. R. Astron. Soc., 18, 51-61, 1969.

Dziewonski, A. M., and D. L. Anderson, Preliminary Reference Earth Model (PREM), Phys. Earth Planet. Inter., 25, 297-356, 1981.

Dziewonski, A. M., and F. Gilbert, The effect of small aspherical perturbations on travel times and a re-examination of the corrections for ellipticity, Geophys. J. R. Astron. Soc., 44, 7-16, 1976.

Dziewonski, A. M., B. H. Hager and R. J. O'Connell, Large-scale heterogeneities in the lower mantle, J. Geophys. Res., 82, 239-255, 1977.

Gutenberg, B., Travel times of longitudinal waves from surface foci, Proc. Natl. Acad. Sci., 39, 849-853, 1953.

Herrin, E., and J. Taggart, Regional variation in P_n velocity and their effect on the location of epicenters, Bull. Seismol. Soc. Am., 52, 1037-1046, 1962.

Herrin, E., and J. Taggart, Regional variations in P travel times, Bull. Seismol. Soc. Am., 58, 1325-1337, 1968.

Herrin, E., W. Tucker, J. Taggart, D. W. Gordon, and J. L. Lobdell, Estimation of surface focus P travel times, Bull. Seismol. Soc. Am., 58, 1273-1291, 1968.

Jeffreys, H., The times of P, S, and SKS and the velocities of P and S, Mon. Not. R. Astron. Soc. Geophys. Suppl., 4, 498-536, 1939.

Jeffreys, H., and K. E. Bullen, Seismological Tables, British Association, Gray-Milne Trust, London, 1940.

Johnson, L. R., Array measurements of P velocities in the upper mantle, J. Geophys. Res., 72, 6309-6325, 1967.

Johnson, L. R., Array measurements of P velocities in the upper mantle, Bull. Seismol. Soc. Am., 59, 973-1008, 1969.

Jordan, T. H., Lithospheric slab penetration into the lower mantle beneath the sea of Okhotsk, J. Geophys., 43, 473-496, 1977.

Julian, B. R., and M. K. Sengupta, Seismic travel time evidence for lateral inhomogeneity in the deep mantle, Nature,242, 443-447, 1973.

Lilwall, R. C., and A. Douglas, Estimation of P wave travel times using the joint epicentre method, Geophys. J. R. Astron. Soc., 19, 165-181, 1970.

Niazi, M. and D. L. Anderson, Upper mantle structure of western North America from apparent velocities of P waves, J. Geophys. Res., 70, 4633-4640, 1965.

Sengupta, M. K., and B. R. Julian, P wave travel times from deep earthquakes, Bull. Seismol. Soc. Am., 66, 1555-1579, 1976.

Toksöz, M. N., M. A. Chinnery, and D. L. Anderson, Inhomogeneities in the earth's mantle, Geophys. J. R. Astron. Soc., 13, 31-59, 1967.

Tucker, W., E. Herrin, and H. W. Freedman, Some statistical aspects of the estimation of seismic travel times, Bull. Seismol. Soc. Am., 58, 1243-1260, 1968.

Vetter, U., and J.-B. Minster, P_n velocity anisotropy in southern California, Bull. Seismol. Soc. Am., 71, 1511-1530, 1981.

Willmore, P. L., and A. M. Bancroft, The time term approach to refraction seismology, Geophys. J. R. Astron. Soc., 3, 419-432, 1960.

Zoback, M. L., and M. Zoback, State of stress in the conterminous United States, J. Geophys. Res., 85, 6113-6156, 1980.

(Received June 14, 1982;
accepted October 22, 1982.)